lymphoma cells derived from *Aml1*$^{+/+}$ *p53*$^{-/-}$ and *Aml1*$^{+/-}$ *p53*$^{-/-}$ mice were positive for T-cell receptor, CD4 and CD8 (Fig. S1a,b). Event-free survival was significantly different between the two genotypes ($P = 0.0325$) (Fig. 1c). These results suggest that expression levels of AML1 affect the incidence of malignancies in p53-null mice.

AML1 is upregulated in cells with p53 aberrations. To determine whether the level of *Aml1* transcripts correlates with the presence or absence of p53, we compared expression of *Aml1* in various types of cells from littermate mice of the *p53*$^{+/-}$ and *p53*$^{-/-}$ genotypes. We observed increased expression of *Aml1* in total bone-marrow (BM) cells, c-Kit^{+} BM cells, common lymphoid progenitors (CLPs), splenic T cells, and thymic T cells, as well as in *p53*$^{-/-}$ mouse embryonic fibroblast (MEF) cells (Fig. 2a–d). Considering that the major function of p53 is regulation of stress-response genes, we tested the effect of stress on the expression of *Aml1* in BM cells from another littermate mouse. *Aml1* is induced by ionizing radiation (IR) in mice with normal *p53*, but this induction was not observed in *p53*$^{-/-}$ cells (Fig. 2e). Levels of *Aml1* expression were increased by p53 shRNA treatment (Fig. S2). Together, these data strongly suggest that *Aml1* is transcriptionally regulated by p53 both in the steady state and following genotoxic stress.

***AML1* is regulated by p53.** There are two promoters in the *AML1* gene.[24] The distal promoter is more active than the proximal promoter in hematopoietic stem cells and developing T cells.[25] To determine whether p53 binds to the distal promoter region of *Aml1*, we performed chromatin immunoprecipitation (ChIP) using c-Kit^{+} cells from mouse BM. For this purpose, we used PCR primers corresponding to regions ranging from −10 kb upstream to +4 kb downstream of the *Aml1* transcription start site (Fig. 3b). When c-Kit^{+} cells were cultured *in vitro*, the expression of *Aml1* was induced (Fig. 3a). Binding of p53 to the *Aml1* promoter could be detected in ChIP analysis before, but not after, cultivation (Fig. 3b). ChIP analysis of histone H3 trimethylated at lysine 4 (H3K4Me3) and histone H3 acetylated at lysine 9 (H3K9Ac), both of which are hallmarks of active gene transcription, indicated that activating modifications of chromatin increased in proportion to the *Aml1* mRNA level. H3 trimethylated at lysine 9 (H3K9Me3), which is a repressive mark, was not altered by the cultivation. These results indicated that, at steady state immediately following the isolation of c-Kit^{+} cells from BM, p53 was preferentially bound close to and downstream of the transcription start site. However, after a 3-day culture of c-Kit^{+} cells, significant binding of p53 was no longer detected at any locus tested (Fig. 3b), even though the expression of p53 was high at this time. At steady state, the *Aml1* distal promoter region appeared to be inactive, as demonstrated by the relatively lower levels of H3K4Me3 and H3K9Ac occupancy revealed by ChIP analysis. Conversely, levels of H3K4Me3 and H3K9Ac increased at the downstream region of the *Aml1* promoter (primers no. 3–5) after a 3-day culture (Fig. 3b and Fig. S3). Occupancy of the *Aml1* promoter by p53 was also decreased following irradiation (Fig. 3c). The results of these ChIP experiments indicate that the activity of the *Aml1* promoter is inhibited by binding of p53 under normal conditions, and that this inhibition was abolished under conditions of stress. In a reporter assay, the *Aml1* promoter was inhibited by wild-type p53 and activated by the p53 R175H mutant, which is defective in binding to DNA (Fig. 4). These results indicate that p53 inhibits transcription of the *Aml1* gene. The p53 R175H mutant may function in a dominant-negative manner.

Depletion of AML1 blocks T-cell proliferation. To determine whether the expression level of AML1 affects proliferation of T cells, we mated mutant animals carrying *lox*P-flanked (*Aml1*^{fl}) alleles[20] with *ERT2-Cre* knock-in mice[21] to generate *Aml1*$^{fl/fl}$ *ERT2-Cre* mice. In these mice, the *Aml1*^{fl} allele

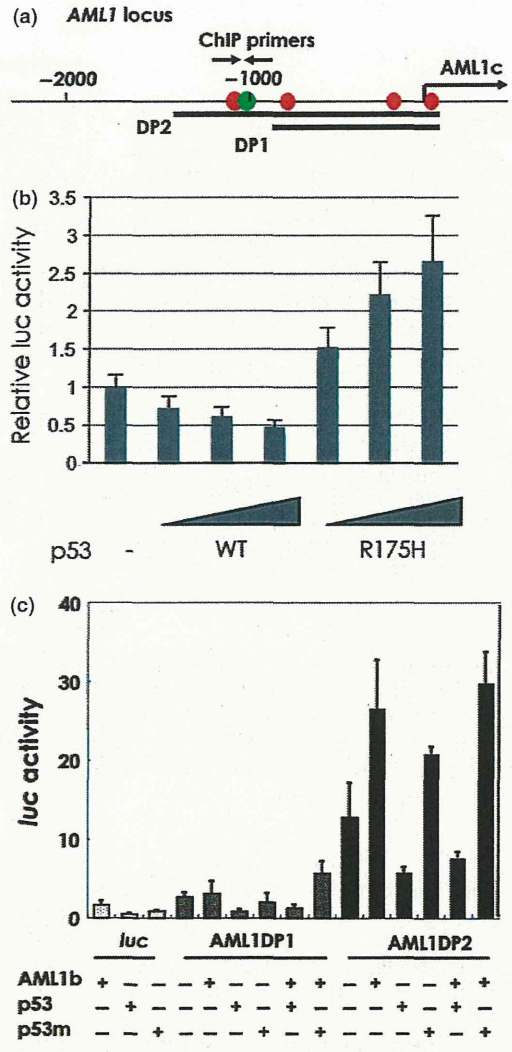

Fig. 4. p53 inactivates *AML1* promoter. (a) The indicated promoter regions of 900 bp (DP1) and 1400 bp (DP2) were cloned into *luc* reporter plasmids. The arrow labeled AML1c indicates the transcription start site. The opposing arrows indicate the positions of the primers used for ChIP analysis. (b, c) AML1 promoter is repressed by p53. SaOs2 cells were transfected with expression vector for wild-type p53, p53R175H and/or AML1b together with a human *AML1* distal promoter–luciferase (*luc*) reporter containing DP1 or DP2. Data shown are relative values of firefly luciferase activity normalized to *Renilla* luciferase activity. The data shown are the means ± standard error of the mean (SEM).

could be effectively deleted *in vitro* in hematopoietic cells by the addition of 4-hydroxytamoxifen (4-OHT), which activates ERT-Cre recombinase (Fig. 5a). After 5 days of 4-OHT treatment, the *Aml1* gene was deleted from almost all cells (Fig. 5b), and the *Aml1* transcript was also almost completely absent, as determined by RT-PCR (Fig. 5c). At this time, the expression level of Runx3, which might compensate for loss of AML1 function, was not altered (Fig. S4). We then examined T-cell proliferation in these *Aml1*$^{fl/fl}$ *ERT2-Cre* mice. Splenic CD4 cells were isolated from the *Aml1*$^{fl/fl}$ *ERT2-Cre* mice and cultured in the presence of IL-2 after stimulation with anti-CD3e. Ten days after the addition of 4-OHT, we compared the number of live cells from *Aml1*$^{fl/fl}$ *ERT2-Cre* and *Aml1*$^{w/w}$ *ERT2-Cre* mice. The proliferation of T-cells from

doi: 10.1111/cas.12199

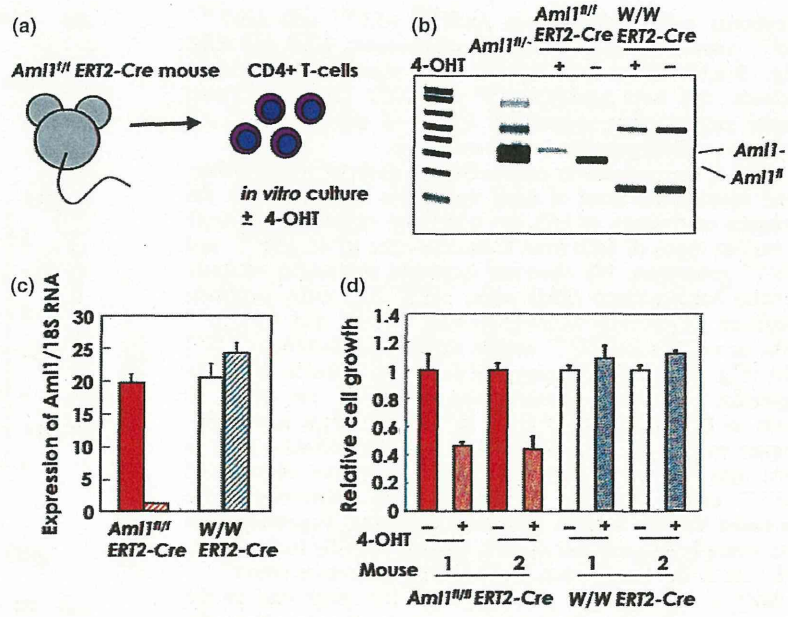

Fig. 5. Depletion of AML1 inhibits the growth of CD4 positive T-cells. (a) Splenic T-cells of *Aml1* $^{fl/fl}$ *ERT2-Cre* mice were isolated using an antibody against CD4 and cultured for 5 days with or without 4-hydroxytamoxifen (4-OHT) in the presence of IL-2. (b) Genotype of *Aml1* was analyzed after 5-day culture with or without 4-OHT in the presence of IL-2. Primers used for genotyping were as follows: f2: ACAAAACCTAGGTGTACCAGGAGAACAAGT, r1: GTCTACTCCTTGCCTCAGAAAACAAAAAC, fl20: CCCT GAAGACAGGAGAAGTTTCCA. (c) Expression of *Aml1* was measured by quantitative reverse transcription-polymerase chain reaction (qRT-PCR) and correlated to *18S* rRNA levels after 5-day culture with or without 4-OHT in the presence of IL-2. (d) T-cells with or without the Aml1 allele were cultured in the presence of IL-2 for 10 days. The growth rate (live cells) was measured by the production of adenosine triphosphate (ATP). ATP production of cells from *Aml1* $^{fl/fl}$ *ERT2-Cre* mice (red bars, diagonal stripe) treated with 4-OHT was less than that of untreated cells (red bars, filled). The drug was not toxic to wild-type cells (white and gray diagonal stripes: treated and non-treated, respectively).

which *Aml1* was deleted was clearly lower than that of T-cells from *Aml1* $^{w/w}$ *ERT2-Cre* mice (Fig. 5d). This result is consistent with a previous report showing that conditional deletion of *Aml1* results in decreased numbers of T cells.[20] These observations suggest an important role for AML1 in T-cell proliferation.

Discussion

RUNX family members function as oncogenes when they are ectopically overexpressed.[26–29] In this study, we elucidated a novel relationship between AML1 and p53 *in vivo* using mice that carried mutations in one or both genes, and we present genetic evidence for a mechanism underlying the overexpression of AML1.

The lower frequency of onset of T-cell lymphoma in association with the *Aml1* $^{+/-}$ *p53* $^{-/-}$ genotype may indicate that the presence of two copies of the *Aml1* gene are needed for T-cell transformation and/or proliferation, and that one allele of *Aml1* confers no growth advantage to malignant cells. Because we did not examine the expression level of *Aml1* at the early stage of T-cell transformation, we cannot fully resolve the importance of AML1 in T-cell malignancy. Moreover, a genetic defect in p53 affects the regulation of a large number of genes. Therefore, *Aml1* hemizygosity might not be the factor that directly prevents malignant transformation in a p53-null background.

Aml1 might function as an oncogene in a lymphoma that develops due to a defect in *p53*. Consistent with this idea, expression levels of *Aml1* were higher in *p53* $^{-/-}$ lymphocytes than those observed in wild type cells (Fig. 2c,d). However, expression levels of *Aml1* were not constantly high in lymphomas (Fig. 1b). These results suggest that high levels of *Aml1* expression might be important for development, but not for maintenance, of lymphomas. The mechanism of this enhanced expression of *Aml1* remains unclear, although the data support the hypothesis that a high level of *Aml1* is critical for lymphoma development. In addition, the depletion or deletion of *Aml1* induced the expression of *Fas* (Fig. S5), suggesting that AML1 plays some roles in cell survival, as reported.[30] In the early stages of lymphoma development, anti-apoptotic regulation by AML1 might also be important.

The primary role of p53 in the cell-cycle checkpoint in hematopoietic cells is probably to repress stem cell division, thereby maintaining the quiescent status of these cells in the steady state.[16] Another recent report also indicated that the reduced p53 activity of *p53* $^{+/-}$ mice is associated with higher numbers of proliferating hematopoietic stem and progenitor cells in older mice.[15] Furthermore, a p53-null genotype promotes expansion of long-term proliferating stem cells in BM and activates HSCs.[15,16] However, the target of p53 that induces HSC proliferation is unknown. Here we showed that AML1 is at least one of the targets of p53 in hematopoietic stem or progenitor cells. AML1 plays a positive role in cell-cycle progression in mouse myeloid cells.[31,32] Thus, the data in this study indicates that p53 may repress AML1 in HSCs in the steady state, but induce AML1 once HSCs are exposed to stress.

The mechanism by which p53 represses *AML1* gene expression may differ from the known mechanisms by which p53 regulates other genes. Our results support a novel mechanism of p53 gene regulation, in which p53 binding to the target-gene locus represses transcription, but release of p53 activates transcription. The ability of p53 to respond to stress is usually associated with modification of p53 by phosphorylation, acetylation, or sumoylation.[33,34] However, it is difficult to use this model to explain our results concerning the stress response of p53 and *AML1* transcription, because p53 normally represses the *AML1* gene but activates it when the cell is exposed to various stresses. We also observed constitutive activation of *AML1* gene in cells with a p53-null genotype. It is likely that, once activated (and probably modified), p53 dissociates from the repressor complex on the *Aml1* gene locus.

In future studies, it will be important to analyze the AML1 level in human T-ALL specimens caused by p53 deficiency or mutation. AML1 has important functions not only in hematopoiesis, but also in neurogenesis and skeletal muscle.[23,35,36] Therefore, a broad-based study of the relationship between the two important transcription factors p53 and AML1 in various malignant diseases could provide information that would aid in understanding how these tumors are generated. If the same results are obtained in human hematopoietic stem cells as in mouse cells, then it may be possible to design drugs that inhibit AML1 activity for use in treating T-cell malignancy.

Acknowledgments

We thank Dr T. Okuda for providing *Aml1* knockout mice, Dr H. Koseki for *Trp53* knockout mice, and Dr M. Enari for the sh-p53 plasmid. We acknowledge C. Hatanaka and M. Shino for technical assistance. We also thank Dr T. Katsumoto and Dr K. Yamagata for technical instruction. This work was supported in part by Grants-in-Aid for Scientific Research from the Ministry of Health, Labor, and Welfare and from the Ministry of Education, Culture, Sports, Science, and Technology, and by the National Cancer Center Research and Development Fund.

Disclosure Statement

The authors have no conflict of interest.

References

1 Miyoshi H, Shimizu K, Kozu T, Maseki N, Kaneko Y, Ohki M. t(8;21) breakpoints on chromosome 21 in acute myeloid leukemia are clustered within a limited region of a single gene, AML1. *Proc Natl Acad Sci USA* 1991; **88**: 10431–4.
2 Golub TR, Barker GF, Bohlander SK *et al.* Fusion of the TEL gene on 12p13 to the AML1 gene on 21q22 in acute lymphoblastic leukemia. *Proc Natl Acad Sci USA* 1995; **92**: 4917–21.
3 Osato M, Asou N, Abdalla E *et al.* Biallelic and heterozygous point mutations in the runt domain of the AML1/PEBP2alphaB gene associated with myeloblastic leukemias. *Blood* 1999; **93**: 1817–24.
4 Imai Y, Kurokawa M, Izutsu K *et al.* Mutations of the AML1 gene in myelodysplastic syndrome and their functional implications in leukemogenesis. *Blood* 2000; **96**: 3154–60.
5 Song WJ, Sullivan MG, Legare RD *et al.* Haploinsufficiency of CBFA2 causes familial thrombocytopenia with propensity to develop acute myelogenous leukaemia. *Nat Genet* 1999; **23**: 166–75.
6 Niini T, Kanerva J, Vettenranta K, Saarinen-Pihkala UM, Knuutila S. AML1 gene amplification: a novel finding in childhood acute lymphoblastic leukemia. *Haematologica* 2000; **85**: 166–75.
7 Dal Cin P, Atkins L, Ford C *et al.* Amplification of AML1 in childhood acute lymphoblastic leukemias. *Genes Chromosom Cancer* 2001; **30**: 407–9.
8 Mikhail FM, Serry KA, Hatem N *et al.* AML1 gene overexpression in childhood acute lymphoblastic leukemia. *Leukemia* 2002; **16**: 658–68.
9 Harewood L, Robinson1 H, Harris R *et al.* Amplification of AML1 on a duplicated chromosome 21 in acute lymphoblastic leukemia: a study of 20 cases. *Leukemia* 2003; **17**: 547–53.
10 Soulier J, Trakhtenbrot L, Najfeld V *et al.* Amplification of band q22 of chromosome 21, including AML1, in older children with acute lymphoblastic leukemia: an emerging molecular cytogenetic subgroup. *Leukemia* 2003; **17**: 1679–82.
11 Vousden KH, Lane DP. p53 in health and disease. *Nat Rev Mol Cell Biol* 2007; **8**: 275–83.
12 Shounan Y, Dolnikov A, MacKenzie KL, Miller M, Chan YY, Symonds G. Retroviral transduction of hematopoietic progenitor cells with mutant p53 promotes survival and proliferation, modifies differentiation potential and inhibits apoptosis. *Leukemia* 1996; **10**: 1619–28.
13 Shaulsky G, Goldfinger N, Peled A, Rotter V. Involvement of wild-type p53 in pre-B-cell differentiation *in vitro*. *Proc Natl Acad Sci USA* 1991; **88**: 8982–6.
14 Kastan MB, Radin AI, Kuerbitz SJ *et al.* Levels of p53 protein increase with maturation in human hematopoietic cells. *Cancer Res* 1991; **51**: 4279–86.
15 Dumble M, Moore L, Chambers SM *et al.* The impact of altered p53 dosage on hematopoietic stem cell dynamics during aging. *Blood* 2007; **109**: 1736–42.
16 Liu Y, Elf SE, Miyata Y *et al.* p53 regulates hematopoietic stem cell quiescence. *Cell Stem Cell* 2009; **4**: 37–48.
17 Prokocimer M, Rotter V. Structure and function of p53 in normal cells and their aberrations in cancer cells: projection on the hematologic cell lineages. *Blood* 1994; **84**: 2391–411.
18 Hatta Y, Yamada Y, Tomonaga M, Said JW, Miyosi I, Koeffler HP. Allelotype analysis of adult T-Cell leukemia. *Blood* 1998; **92**: 2113–7.
19 Jacks T, Remington L, Williams BO *et al.* Tumor spectrum analysis in p53-mutant mice. *Curr Biol* 1994; **4**: 1–7.
20 Ichikawa M, Asai T, Saito T *et al.* AML-1 is required for megakaryocytic maturation and lymphocytic differentiation, but not for maintenance of hematopoietic stem cells in adult hematopoiesis. *Nat Med* 2004; **10**: 299–304.
21 Seibler J, Zevnik B, Küter-Luks B. Rapid generation of inducible mouse mutants. *Nucleic Acids Res* 2003; **31**: e12.
22 Alberts AS, Geneste O, Treisman R. Activation of SRF-Regulated chromosomal templates by Rho-family GTPases requires a signal that also induces H4 hyperacetylation. *Cell* 1998; **92**: 475–87.
23 Okuda T, van Deursen J, Hiebert SW, Grosveld G, Downing JR. AML1, the target of multiple chromosomal translocations in human leukemia, is essential for normal fetal liver hematopoiesis. *Cell* 1996; **84**: 321–30.
24 Miyoshi H, Ohira M, Shimizu K *et al.* Alternative splicing and genomic structure of the AML1 gene involved in acute myeloid leukemia. *Nucleic Acids Res* 1995; **23**: 2762–9.
25 Telfer JC, Rothenberg EV. Expression and function of a stem cell promoter for the murine CBFalpha2 gene: distinct roles and regulation in natural killer and T cell development. *Dev Biol* 2001; **229**: 363–82.
26 Wotton SF, Blyth K, Kilbey A *et al.* RUNX1 transformation of primary embryonic fibroblasts is revealed in the absence of p53. *Oncogene* 2004; **23**: 5476–86.
27 Kurokawa M, Tanaka T, Tanaka K *et al.* Overexpression of the AML1 proto oncoprotein in NIH3T3 cells leads to neoplastic transformation depending on the DNA-binding and transactivation potencies. *Oncogene* 1996; **12**: 883–92.
28 Wotton SF, Stewart M, Blyth K *et al.* Proviral insertion indicates a dominant oncogenic role for Runx1/AML-1 in T-cell lymphoma. *Cancer Res* 2002; **62**: 7181–5.
29 Blyth K, Terry A, Mackay N *et al.* Runx2: a novel oncogenic effector revealed by *in vivo* complementation and retroviral tagging. *Oncogene* 2001; **20**: 295–302.
30 Fujii M, Hayashi K, Niki M *et al.* Overexpression of AML1 renders a T hybridoma resistant to T cell receptor-mediated apoptosis. *Oncogene* 1998; **17**: 1813–20.
31 Bernardin-Fried F, Kummalue T, Leijen S, Collector MI, Ravid K, Friedoman AD. AML1/RUNX1 increases during G1 to S cell-cycle progression independent of cytokine-dependent phosphorylation and induces cyclin D3 gene expression. *J Biol Chem* 2004; **279**: 15678–87.
32 Growney JD, Shigematsu H, Li Z *et al.* Loss of Runx1 perturbs adult hematopoiesis and is associated with a myeloproliferative phenotype. *Blood* 2005; **106**: 494–504.
33 Bode AM, Dong Z. Post-translational modification of p53 in tumorigenesis. *Nat Rev Cancer* 2004; **4**: 793–805.
34 Dai C, Gu W. p53 post-translational modification: deregulated in tumorigenesis. *Trends Mol Med* 2010; **16**: 528–36.
35 Theriault FM, Roy P, Stifani S. AML1/Runx1 is important for the development of hindbrain cholinergic branchiovisceral motor neurons and selected cranial sensory neurons. *Proc Natl Acad Sci USA* 2004; **101**: 10343–8.
36 Wang X, Blagden C, Fan J *et al.* Runx1 prevents wasting, myofibrillar disorganization, and autophagy of skeletal muscle. *Genes Dev* 2005; **19**: 1715–22.

Supporting Information

Additional Supporting Information may be found in the online version of this article:

Fig. S1. Phenotypes of lymphomas.

Fig. S2. Effects of p53 shRNA on AML1 expression.

Fig. S3. Active chromatin modifications in the distal promoter regions of the mouse and human *AML1* genes.

Fig. S4. Effect of AML1 depletion on the *Runx3* gene expression.

Fig. S5. Effect of AML1 depletion on *Fas* gene expression.

Table S1. Type of diseases and latency seen in p53-null mice.

doi: 10.1111/cas.12199

OPEN ACCESS Freely available online

PLOS | ONE

MLL Becomes Functional through Intra-Molecular Interaction Not by Proteolytic Processing

Akihiko Yokoyama[1]*, Francesca Ficara[2,3], Mark J. Murphy[4], Christian Meisel[5], Chikako Hatanaka[6], Issay Kitabayashi[6], Michael L. Cleary[4]*

1 Laboratory for Malignancy Control Research, Kyoto University Graduate School of Medicine, Kyoto, Japan, **2** Milan Unit, Istituto di Ricerca Genetica e Biomedica, Consiglio Nazionale delle Ricerche, Milan, Italy, **3** Humanitas Clinical and Research Center, Rozzano, Italy, **4** Department of Pathology, Stanford University School of Medicine, Stanford, California, United States of America, **5** Depertment of Neurology, University Clinic Carl Gustav Craus, Dresden, Germany, **6** Division of Hematological Malignancy, National Cancer Center Research Institute, Tokyo, Japan

Abstract

The mixed lineage leukemia (MLL) protein is an epigenetic transcriptional regulator that controls proliferative expansion of immature hematopoietic progenitors, whose aberrant activation triggers leukemogenesis. A mature MLL protein is produced by formation of an intra-molecular complex and proteolytic cleavage. However the biological significance of these two post-transcriptional events remains unclear. To address their in vivo roles, mouse mutant alleles were created that exclusively express either a variant protein incapable of intra-molecular interaction (designated *de*) or an uncleavable mutant protein (designated *uc*). The *de* homozygous mice died during midgestation and manifested devastating failure in embryonic development and reduced numbers of hematopoietic progenitors, whereas *uc* homozygous mice displayed no apparent defects. Expression of MLL target genes was severely impaired in *de* homozygous fibroblasts but unaffected in *uc* homozygous fibroblasts. These results unequivocally demonstrate that intra-molecular complex formation is a crucial maturation step whereas proteolytic cleavage is dispensable for MLL-dependent gene activation and proliferation in vivo.

Citation: Yokoyama A, Ficara F, Murphy MJ, Meisel C, Hatanaka C, et al. (2013) MLL Becomes Functional through Intra-Molecular Interaction Not by Proteolytic Processing. PLoS ONE 8(9): e73649. doi:10.1371/journal.pone.0073649

Editor: Tadayuki Akagi, Kanazawa University, Japan

Received June 5, 2013; **Accepted** July 21, 2013; **Published** September 10, 2013

Funding: These studies were supported by a Grant-in-aid for Young Scientists (A)(23689050) and a Grant-in-aid for Scientific Research on Innovative Areas from Japan Society for the promotion of Science (22118003) to A.Y., and a grant from the National Institutes of Health to M.L.C. (CA116606). F.F, was supported by a Scholar Award from the American Society of Hematology (http://www.hematology.org). The funders had no role in study design, data collection and analysis, decision to publish, or preparation of the manuscript.

Competing Interests: The authors have declared that no competing interests exist.

* E-mail: yokoyama@dsk.med.kyoto-u.ac.jp (AY); mcleary@stanford.edu (MLC)

Introduction

MLL (also known as MLL1, HRX and KMT2A) is an epigenetic transcriptional regulator that serves essential roles in embryonic and hematopoietic development. During embryogenesis, MLL maintains expression of Homeobox (*HOX*) genes to confer cellular identities along the anterior-posterior body axis [1], [2]. In the hematopoietic lineage, MLL regulates expression of a subset of *HOX* genes [3], [4] that promotes self-renewal of hematopoietic stem cells (HSCs) and expansion of immature progenitor pools [5], [6]. Hence, *Mll* deficiency in mice causes hematopoietic failure accompanied with insufficient expansion of immature hematopoietic progenitors [3], [7], [8]. Furthermore, *MLL* suppresses premature-senescence in both human and mouse fibroblasts in part by maintaining *HOX* gene expression [8], [9], [10]. Therefore loss of MLL function causes premature senescence. Conversely, *MLL* gain-of-function mutations caused by chromosomal translocations in hematopoietic cells result in constitutive expression of *HOX* genes that aberrantly enhance proliferation [11], [12] and suppress senescence to cause acute leukemia [8], [10].

MLL is translated as a large precursor protein (430 kD) that subsequently undergoes proteolytic processing into two fragments (MLL^N and MLL^C) by the Taspase 1 endopeptidase [13], [14], [15], which specifically cleaves sites that are evolutionally conserved with MLL2 (also known as MLL4, HRX2 and KMT2B) and Drosophila TRX. The respective MLL^N and MLL^C fragments form a holocomplex by non-covalent intra-molecular interaction [14], [15]. Although these MLL fragments are susceptible to distinct degradation pathways [8], the MLL^N/MLL^C holocomplex is stably expressed because intra-molecular complex formation masks structures that would otherwise lead to degradation. However, the biological significance of these maturation processes in vivo remains unclear.

In the current study, the in vivo roles of intra-molecular complex formation and proteolytic processing in MLL functions were examined using knock-in mouse lines with targeted mutations that selectively prevent self-association and proteolytic cleavage, respectively.

Materials and Methods

Ethics statement

All animal work has been conducted according to the institutional guidelines with the approval of Stanford University (9839) and National Cancer Center Research Institute (T08-030-N, T08-030-CB02).

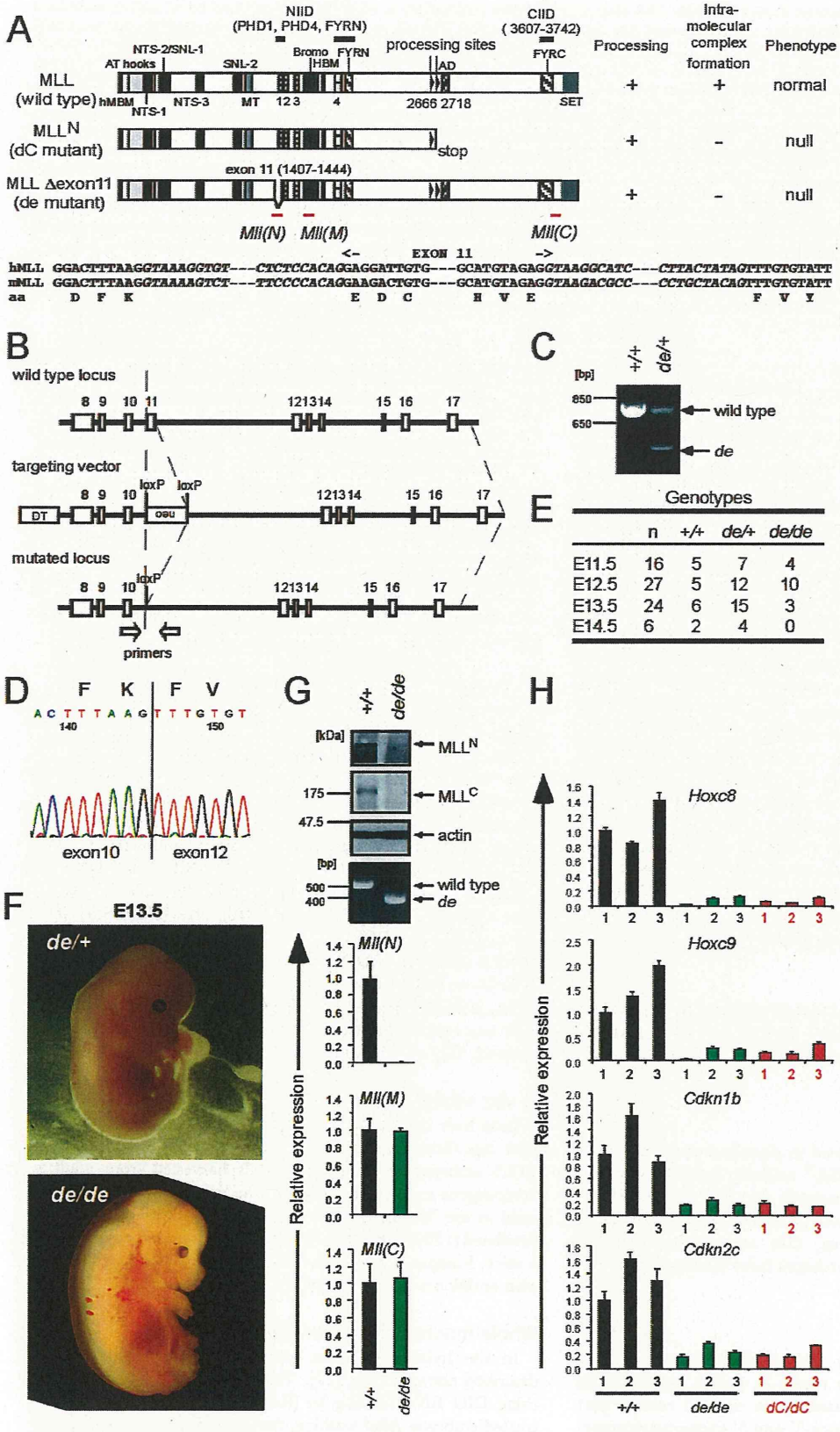
A
NIID
(PHD1, PHD4, FYRN)
CIID
(3607-3742)
processing sites
Processing
Intra-molecular complex formation
Phenotype
NTS-2/SNL-1
AT hooks
SNL-2
Bromo
HBM
FYRN
AD
FYRC
MLL (wild type)
hMBM
NTS-1
NTS-3
MT
123
4
2666 2718
SET
+
+
normal
MLL^N (dC mutant)
stop
+
-
null
exon 11 (1407-1444)
MLL Δexon11 (de mutant)
+
-
null
Mll(N)
Mll(M)
Mll(C)
<-
EXON 11
->
hMLL GGACTTTAAGGTAAAGGTGT---CTCTCCACAGGAGGATTGTG---GCATGTAGAGGTAAGGCATC---CTTACTATAGTTTGTGTATT
mMLL GGACTTTAAGGTAAAAGTCT---TTCCCCACAGGAAGACTGTG---GCATGTAGAGGTAAGACGCC---CCTGCTACAGTTTGTGTATT
aa D F K E D C H V E F V Y
B
wild type locus
8 9 10 11
121314
15 16
17
targeting vector
loxP
loxP
DT
neo
mutated locus
primers
C
[bp]
850
650
+/+
de/+
wild type
de
E
Genotypes
n +/+ de/+ de/de
E11.5 16 5 7 4
E12.5 27 5 12 10
E13.5 24 6 15 3
E14.5 6 2 4 0
D
F K F V
A C T T T A A G T T T G T G T
140
150
exon10
exon12
F
E13.5
de/+
de/de
G
+/+
de/de
[kDa]
MLL^N
175
MLL^C
47.5
actin
[bp]
500
400
wild type
de
Mll(N)
Mll(M)
Mll(C)
Relative expression
+/+
de/de
H
Hoxc8
Hoxc9
Cdkn1b
Cdkn2c
Relative expression
1 2 3 1 2 3 1 2 3
+/+
de/de
dC/dC

Figure 1. Intra-molecular interaction is required for MLL-dependent gene activation. A. MLL proteins produced by *dC* and *de* mutations are shown schematically. The characteristics of each mutant are shown on the right. The N-terminal intra-molecular interaction domain (NIID) includes PHD1, PHD4 and FYRN and the C-terminal intra-molecular interaction domain (CIID) is FYRC. Positions of the three taqman probes for *Mll* [*Mll*(N), *Mll*(M) and *Mll*(C)] used in Figure 1G are indicated by red bars. Genomic sequences around the exon 11 of the human MLL and its murine counterpart are shown at the bottom. B. Genomic structures of the wild type allele and the recombined allele are shown with the targeting vector. C. Diagnostic PCR identifies the recombined allele in genetically engineered mice. +/+: wild type. *de*/+: *de* heterozygous D. Sequence of the exon junction of *Mll de* transcript. The PCR product generated by RT-PCR of *de* homozygous MEFs was sequenced. E. Genotypes at various developmental stages. Viability of embryos was confirmed by presence of heart contractions. *de*/*de*: *de* homozygous F. Morphologies of E13.5 embryos of *de* mutants. G. Expression of MLL proteins and RNAs in MEFs. Expression of MLL^N, MLL^C, and actin was visualized by western blotting. Relative expression levels of *Mll* mRNAs (normalized to *Gapdh*) are expressed relative to those of wild type arbitrarily set as 1. RT-PCR analysis demonstrated expression of the *de* mutant mRNAs. qPCR using the *Mll*(M) and *Mll*(C) taqman probe demonstrated that *Mll* mRNAs were expressed at the same levels in wild type and *de* homozygous MEFs, whereas the *Mll*(N) taqman probe showed that the murine exon corresponding to the human exon 11 was not transcribed. Error bars represent the standard deviations of triplicate PCRs. H. Expression of MLL target genes in *de* homozygous MEFs. Wild type and *dC* homozygous MEFs were also analyzed for comparison. Relative expression levels of various MLL target genes (normalized to *Gapdh*) are expressed relative to those of wild type-1 arbitrarily set as 1. RT-qPCR demonstrates that expression of MLL target genes including *Hoxc8*, *Hoxc9*, *Cdkn1b*, *Cdkn2c* was impaired in *de* homozygous and *dC* homozygous MEFs. Error bars represent the standard deviations of triplicate PCRs. *dC*/*dC*: *dC* homozygous.
doi:10.1371/journal.pone.0073649.g001

Generation of knock-in mice

Targeting vectors containing the mutations and the cassettes of Neomycin resistance gene (neo) and Diphtheria toxin gene (DT) (kindly provided by Dr. Takeshi Yagi) were constructed by PCR-mediated mutagenesis and restriction enzyme digestion/ligation. The targeting vector for the *uc* mutation was constructed in the same manner as the previously published *dC* mutant allele [8]. ES cells (CGR8.8) were transfected with the linearized targeting vectors and screened for positive clones by PCR. Homologous recombination was confirmed by LA-PCR (Takara Bio Inc., Otsu, Japan) using primer pairs specific for both ends of the targeting construct (primer sequences available upon request). Targeted ES clones were transiently transfected with a Cre recombinase expression vector (kindly provided by Dr. Takeshi Yagi) and subsequently screened for clones with appropriate excision of the neo cassette. Blastocyst injections were performed by the Transgenic Research Facility of Stanford University. Knock-in mouse lines were maintained by backcrossing onto a C57BL/6 genetic background. Genotyping of mice for the *de* allele was performed by PCR using a primer set (5′- tgaactggtgggaaagcacacagacatcctga -3′ and 5′-agagatggttcagcggttaagagctctgac-3′) that detected both the mutant allele (~500 bp) and the wild type allele (800 bp). Genotyping of mice for the *uc* allele was performed by PCR using a primer set (5′-gttctgaagcacacattccacacc-3′ and 5′-catcaaagcgaagggcaatcagtg-3′) that detected both the mutant allele (~310 bp) and the wild type allele (250 bp).

Cell culture

293T, plat-E, and mouse embryonic fibroblast (MEF) cells were cultured in Dulbecco's modified Eagle's medium (DMEM) supplemented with 15% fetal calf serum and non-essential amino acids.

Western blotting

Western blotting was performed as described previously [15]. The mouse monoclonal anti-MLL^N antibody (mmN4) and anti-MLL^C antibody (9–12) were previously described [8], [15]. Goat anti-menin antiserum (C19) was purchased from Santa Cruz Biotechnology Inc (Santa Cruz, CA) and mouse anti-actin antibody (MAB 1501R) was purchased from Millipore (Billerica, MA).

RT-PCR

Reverse transcription (RT) was performed as described previously [8]. RT-PCR of the mouse *de* variant transcript was performed using a primer set flanking the exon 11 counter part sequences (5′-agatggagtccacaggatca-3′ and 5′-tttcttcgtgggtttggtgg-3′). Quantitative PCR (qPCR) was performed in triplicate and average expression levels (with standard deviations) normalized to that of *Gapdh* or *Actb* were calculated using a standard curve and the relative quantification method as described in ABI User Bulletin #2. Taqman probes for various genes [*Gapdh*: Mm99999915_g1, *Actb*:Mm00607939_s1, *Mll*(N):Mm0117926_g1, *Mll*(M):Mm01179218_m1, *Mll*(C):Mm10179235_m1, *Hoxc8*:Mm00439369_m1, *Cdkn2a*:Mm00494449_m1, *Cdkn1b*:Mm00438167_g1, *Cdkn2c*:Mm00483243_m1, *Hoxc4*:Mm00442838_m1, *Hoxc9*:Mm00433972_m1, *PAI-1*(*Serpine1*):Mm00435860_m1, *Men1*:Mm00484963_m1, *Ledgf* (*Psip1*):Mm01259222_g1, *Hoxa10*:Mm00433966_m1, *Hoxa9*:Mm00439364_m1, *Hoxa7*:Mm00657963_m1] were purchased from Applied Biosystems (Foster City, CA).

Flow cytometry analysis and sorting

Flow cytometry was performed as previously described [8], [16]. Single cell suspensions harvested from the bone marrow and thymus were stained in deficient RPMI (Irvine Scientific, Santa Ana, CA) containing 3% fetal calf serum, 1 mM EDTA and 10 mM HEPES. Conjugated monoclonal antibodies (mAbs) were obtained from either BD (Flanklin Lakes, NJ) or eBioscience (San Diego, CA). The lineage cocktail included antibodies for Gr1 (RB6-8C5), B220 (RA3-6B2), TER119 (TER-119), CD3 (145-2C12), CD4 (GK1.5), and CD8 (53-6.7). The following mAbs were also used: Mac1/CD11b (M1/70), cKit (2B8), Sca1 (D7), CD48 (HM48-1), CD34 (49E8), CD16/32 (93), Flk2 (A2F10), CD45.2 (104), and CD43 (S7). Stained cells were analyzed with LSR-1A or LSR-II flow cytometer (BD). J-SAN (Bay bioscience, Kobe, JAPAN) was used for cell sorting. Cell Quest Pro or Diva (BD) was used for data acquisition, and FlowJo (Tree Star Inc., Ashland, OR) was used for analysis.

In vivo reconstitution assay

Fetal liver cells of *de* homozygous mutant (5×10^5 cells) or the wild type/heterozygous controls (5×10^4 cells) harvested from E12.5 embryos or white blood cells harvested from adult *uc* homozygous mice (1×10^6 cells) or the wild type control (1×10^6 cells) in the littermates were injected intravenously into lethally irradiated (1200 rads in two days or 900 rads in one day) C57BL/6 mice. Recipient mice were maintained on water supplemented with antibiotics for a few weeks after transplantation.

Whole mount in situ hybridization

In situ hybridization was performed on E10.5 embryos as described elsewhere [8], [17]. The *Hoxc8* probe was synthesized using DIG RNA labeling kit (Roche) and hybridized with pre-treated embryos. After washing, the probe was visualized by anti-

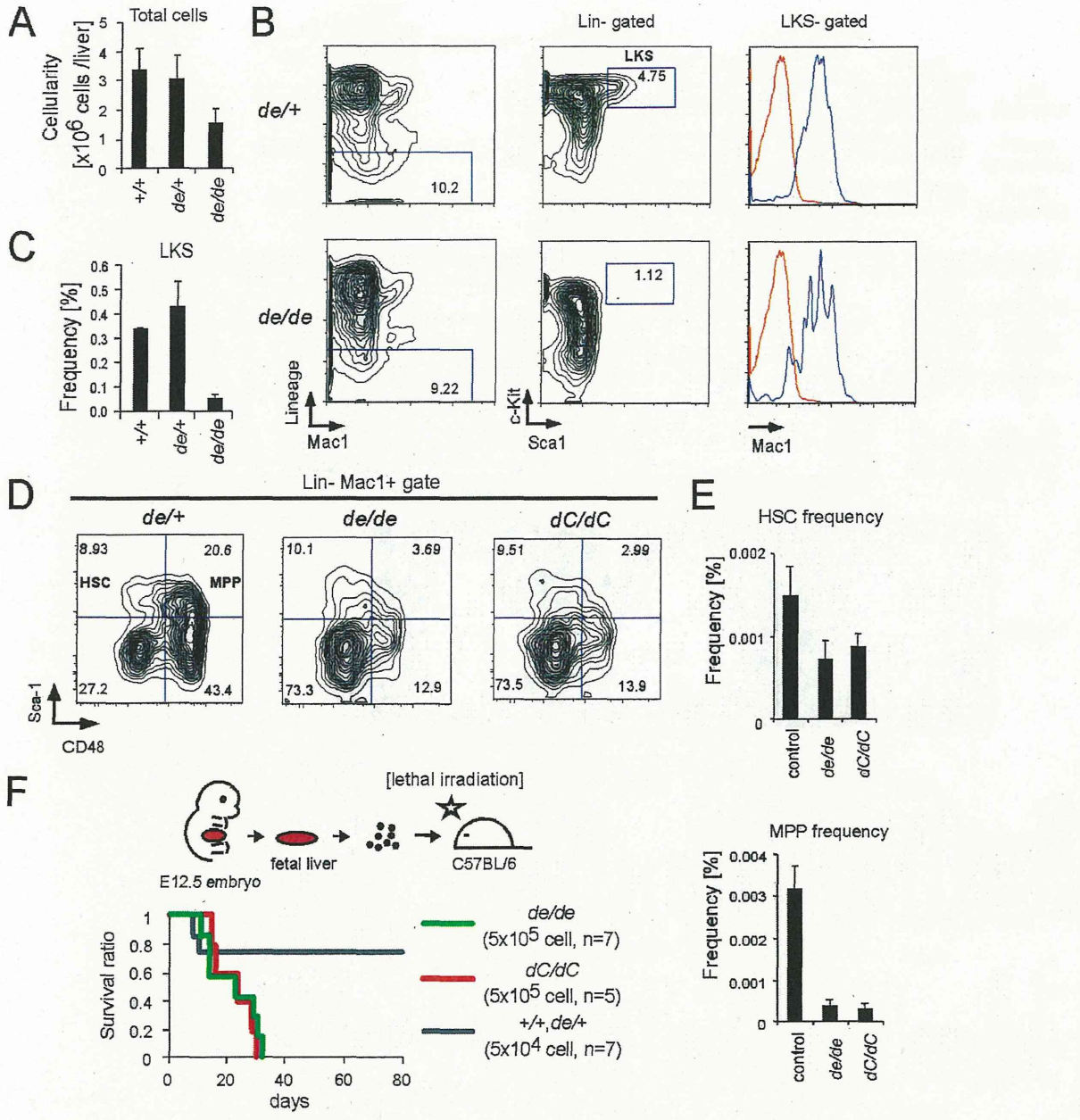

Figure 2. Intra-molecular interaction is required for expansion of hematopoietic progenitors. A. Cellularity of *de* mutant FLs. Error bars represent the standard deviations of cell numbers of FLs. For each genotype, at least 3 livers were analyzed. B. Population analysis of ^{de} mutant FLs by flow cytometry. The fetal LKS compartment was defined as the $Lin^{-}cKit^{+}Sca\text{-}1^{+}Mac1^{+}$ population. C. Frequency of LKS populations in ^{de} mutant FLs. Error bars represent the standard deviations of more than two littermate embryos for each genotype. D. Population analysis of HSCs from MPPs in ^{de} mutant FLs by flow cytometry. $Lin^{-}Mac1^{+}$ cells were subdivided by Sca-1 and CD48. E. Frequencies of HSCs (top) and MPPs (bottom) in ^{de} mutant FLs. Error bars represent the standard deviations of more than four embryos for each genotype. Frequency was expressed as the percentage of each fraction within the whole population. F. Ability of ^{de} mutant FL cells to reconstitute the hematopoietic system. 5×10^5 cells of ^{de} homozygous FLs and 5×10^4 cells of the wild type/heterozygous controls were transplanted into lethally irradiated syngenic mice. Previously published data for ^{dC} homozygous FLs [8] obtained in the same experimental setting were included for comparison. N: the number of FLs analyzed.
doi:10.1371/journal.pone.0073649.g002

digoxygenin antibody coupled with alkaline phosphatase. The plasmid for the *Hoxc8* probe was kindly provided by Dr. Licia Selleri.

MEF proliferation and 3T3 senescence assays

MEFs were derived from E11.5 embryos and analyzed as described elsewhere [8], [18]. The MEFs were plated at the concentration of 10^4 cells/ml on Day 0 and the cell count was

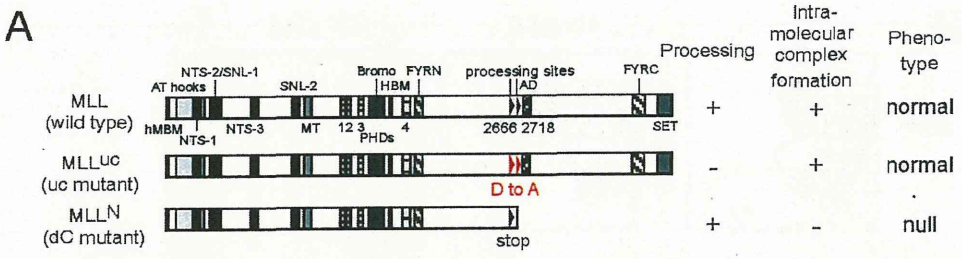

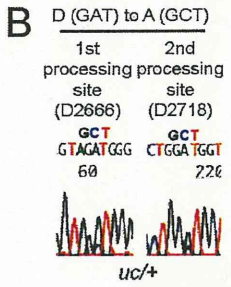

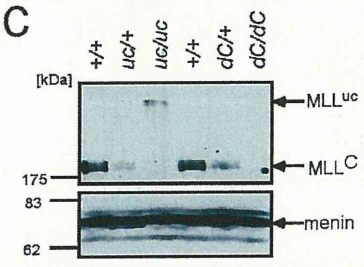

D Genotypes at various developmental stages

	n	+/+	uc/+	uc/uc
E10.5	14	5	5	4
E11.5	20	6	9	5
E12.5	37	9	19	9
E13.5	16	5	6	5
E14.5	20	5	10	5
new born	23	5	10	8
4 weeks old	65	11	38	16

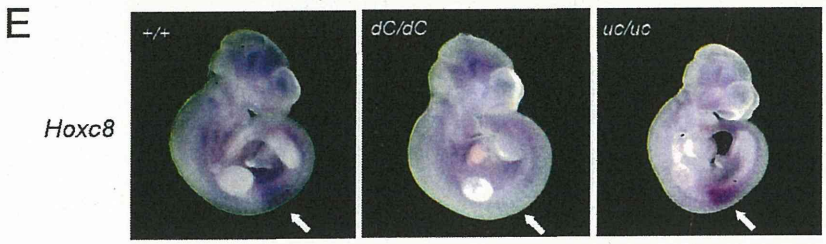

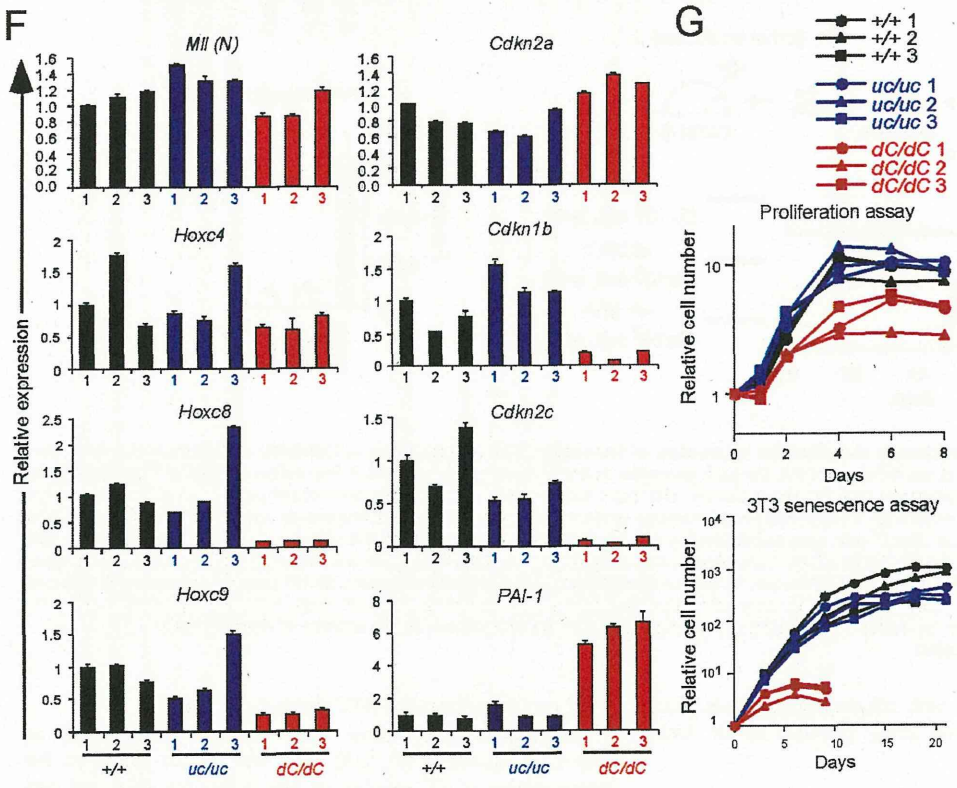

Figure 3. MLL processing is not required for MLL-dependent gene activation. A. Schematic structures of MLL proteins produced by *dC* and *uc* mutations. The characteristics of each mutant are shown on the right. The mutated processing sites are highlighted in red. B. Sequences at the processing sites of the PCR fragments amplified from genomic DNAs of the recombined ES cell clones. C. Expression of MLL proteins in embryos. Western blotting was performed on whole embryo extracts of various genotypes. MLL proteins were visualized by anti-MLL^C antibody. Anti-menin blot serves as a loading control. *uc/+*: *uc* heterozygous. *uc/uc*: *uc* homozygous. *dC/+*: *dC* heterozygous. *dC/ dC*: *dC* homozygous. D. Genotypes at various developmental stages. Viability of embryos was confirmed by presence of heart contractions. E. Expression of *Hoxc8* transcripts in E10.5 embryos. Whole mount in situ hybridization was performed using the *Hoxc8* probe *(Hoxc8)*. Arrows indicate sites of target gene expression. Previously published data for the wild type and *dC* homozygous embryos [8] are shown here for comparison. F. Expression of various genes in mutant MEFs. Three independently established MEF lines of wild type, *uc* homozygous and *dC* homozygous genotypes were examined by RT-qPCR for genes indicated at the tops of respective panels. Relative expression levels (normalized to *Gapdh*) are expressed relative to those of wild type-1 arbitrarily set as 1. Previously published data for wild type and *dC* homozygous MEFs [8] obtained in the same experiment are included for comparison. Error bars represent the standard deviations of triplicate PCRs. G. Proliferative capacities of *uc* homozygous MEFs. Proliferation assay (top) and 3T3 senescence assay (bottom) were performed for three lines each of wild type, *uc* homozygous and *dC* homozygous genotypes at passage 3. Previously published data for wild type and *dC* homozygous MEFs [8] obtained in the same experiments are included for comparison.
doi:10.1371/journal.pone.0073649.g003

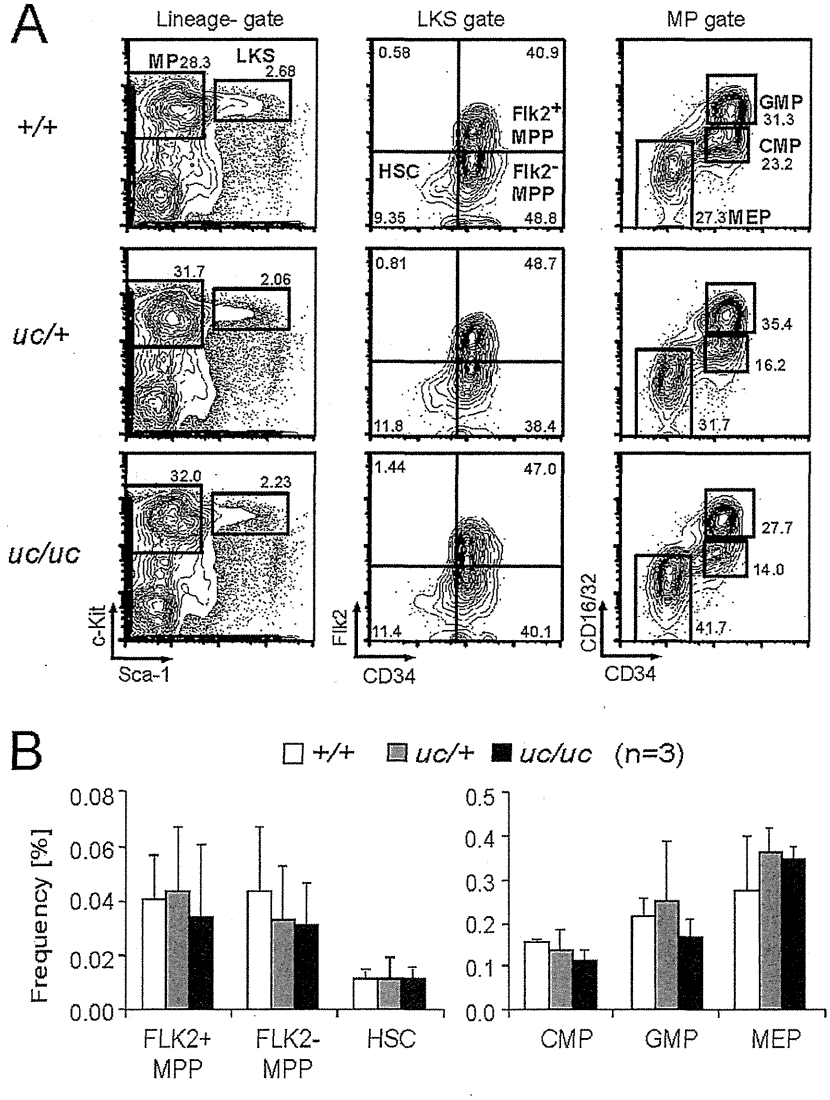

Figure 4. Processing of MLL is not required for adult hematopoiesis. A. Population analysis of Lin$^-$cKit$^+$Sca1$^-$ (MP) and Lin$^-$cKit$^+$Sca1$^+$ (LKS) compartments and their subcompartments in the BM of adult *uc* mutant mice. Lineage cocktail (anti-CD3, CD4, CD8, B220, TER119, Gr-1, Mac1/CD11b) was used to define lineage negative fractions. B. Frequencies of hematopoietic progenitors (Flk2$^-$MPP, Flk2$^+$MPP, CMP, GMP and MEP) and HSCs in *uc* mutant mice. Error bar represents standard deviations of three independent samples.
doi:10.1371/journal.pone.0073649.g004

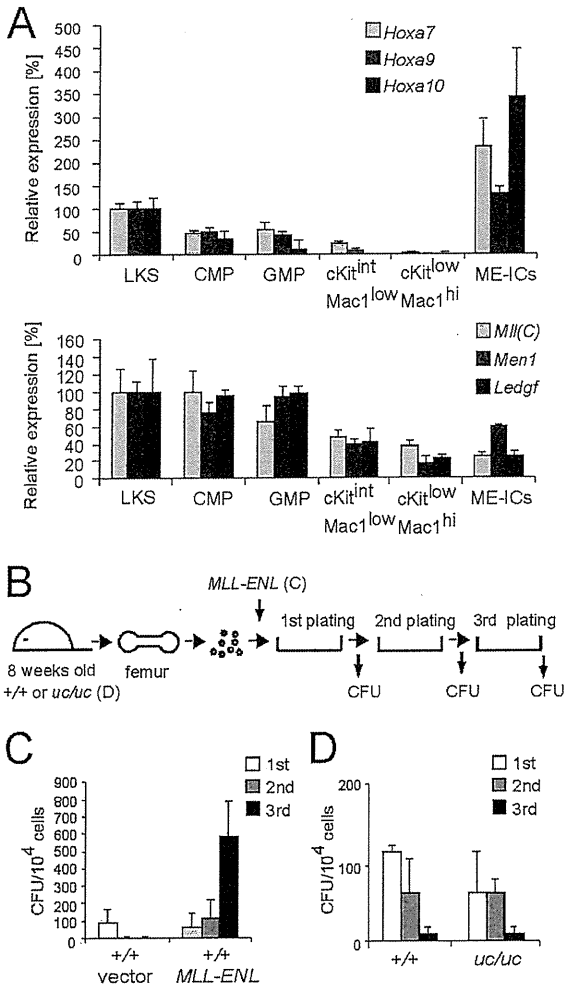

Figure 5. Lack of processing does not constitutively activate MLL. A. Expression of posterior *Hoxa* genes and MLL complex components during myeloid differentiation. Each population was isolated by cell sorting and analyzed by RT-qPCR. Relative expression levels (normalized to *Actb*) and expressed relative to those of LKS arbitrarily set as 100%. Error bars represent standard deviations of triplicate PCRs. B. Experimental scheme of myeloid progenitor serial replating assay. *MLL-ENL* was transduced into wild type myeloid progenitors in Figure 5C. Colony-forming activity of wild type and *uc* homozygous myeloid progenitors was analyzed without any gene transduction in Figure 5D. C. Clonogenic potentials of *MLL-ENL* (or vector)-transduced myeloid progenitors in myeloid progenitor serial replating assay. Transduced cells were cultured in semi-solid media and subjected to serial replating. CFUs per 10^4 plated cells were enumerated after each round. Error bars represent standard deviations of three independent samples. D. Clonogenic potentials of myeloid progenitors derived from *uc* homozygous mice in myeloid progenitor serial replating assay. Error bars represent standard deviations of three independent samples.
doi:10.1371/journal.pone.0073649.g005

measured at each time point. In 3T3 senescence assay, the MEFs were re-plated every 3 days.

Myeloid progenitor serial replating assay

Myeloid progenitor serial replating assay was described elsewhere [19], [20]. Myeloid progenitor cells were harvested from the femurs of mice. C-kit positive cells were enriched by immuno-magnetic selection using an Auto MACS (Miltenyi Biotech), transduced with recombinant retrovirus by spinoculation, and plated in methylcellulose medium (M3231, Stemcell Technologies) containing SCF, IL-3, IL-6 and GM-CSF. The colony-forming units (CFUs) per 10^4 plated cells were quantified after 5–7 d of culture and expressed as the average and standard deviation of at least triplicate determinations.

Results

Intra-molecular complex formation of MLL fragments is essential for MLL-dependent gene activation

The intra-molecular interaction domains of MLL have been defined as PHD fingers 1 and 4 (PHD1 and PHD4), FYRN, and FYRC domains [8], [15] (Figure 1A). Most of PHD1 is encoded by exon 11 of MLL. It has been reported that an MLL variant protein lacking exon 11 sequences is dominantly expressed in some cases of acute lymphoid leukemia [21]. We previously reported that this variant protein can be transiently expressed and efficiently processed but is incapable of forming an MLL^N/ MLL^C holocomplex [8]. To investigate the in vivo roles of intra-molecular complex formation, a mutant allele (designated *de*) that lacks the exon 11 counterpart of mouse was generated in ES cells (Figure 1B) and its successful recombination was confirmed by diagnostic genomic PCR (Figure 1C) and RT-PCR followed by sequencing (Figure 1D). Another mutant allele (designated *dC*), which served as a control for null mutation, was previously engineered to contain a stop codon at the second processing site [8], thereby exclusively expressing MLL^N due to the inability to translate downstream MLL^C sequences within the *Mll* mRNA (Figure 1A).

Unlike wild type and *de* heterozygous mice, *de* homozygous mice died during midgestation (Figure 1E) with a similar phenotype displayed by *dC* homozygous (*dC/dC*) mice [8], including subcutaneous edema and hemorrhage (Figure 1F). Mouse embryonic fibroblasts (MEFs) derived from *de* homozygous embryos expressed MLL proteins at low or undetectable levels whereas their respective mRNAs were expressed at normal levels (Figure 1G), confirming previous findings that MLL protein fragments are subjected to degradation if unable to self-associate in an intra-molecular complex [8], [14]. Consequently, expression of MLL target genes including *Hoxc8*, *Hoxc9*, *Cdkn1b* and *Cdkn2c* was severely reduced in *de* homozygous MEFs [22], [23] (Figure 1H). These results clearly demonstrate that intra-molecular complex formation is required for stable expression of MLL proteins and thus for MLL-dependent gene activation in vivo.

Intra-molecular complex formation is required for expansion of hematopoietic progenitors

The effect of intra-molecular complex formation on proliferative expansion of hematopoietic progenitors was examined by flow cytometry analysis of the fetal livers (FLs) derived from *de* homozygous E12.5 embryos, which contained fewer hematopoietic cells compared to the wild type/heterozygous control FLs (Figure 2A). The LKS compartment, which contains HSCs and multi-potent progenitors (MPPs), was markedly reduced in *de* homozygous FLs (Figure 2B, 2C). Further analysis using the CD48 marker [24] showed that *de* homozygous FLs produced HSCs 50% less efficiently than the wild type/heterozygous controls (Figure 2D, 2E). MPP frequency was more profoundly affected by loss of intra-molecular complex formation, phenocopying *dC* homozygous FLs [8]. Transplantation of FL cells into lethally irradiated mice showed that *de* homozygous FL cells were unable to reconstitute

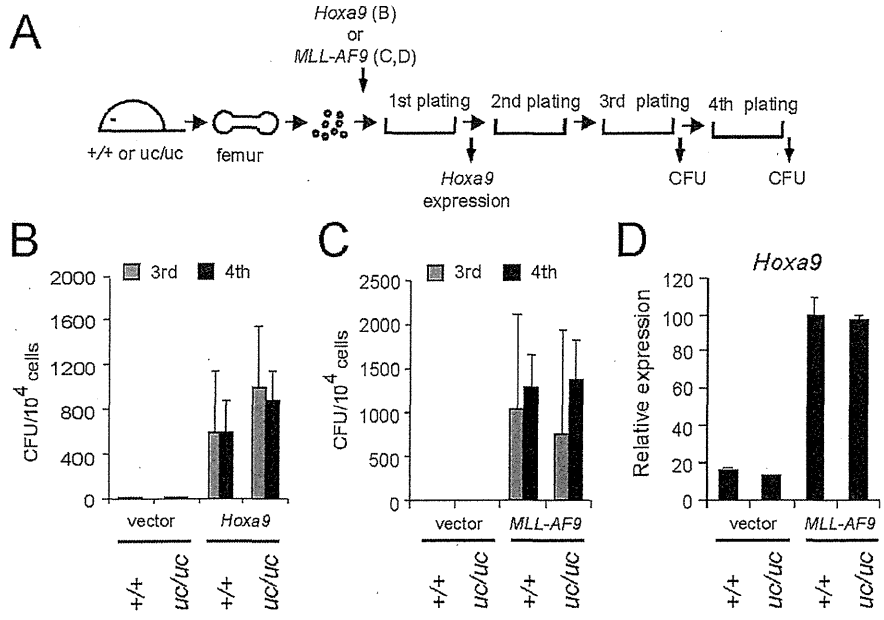

Figure 6. MLL processing is not required for proliferation of oncogene-transformed myeloid progenitors. A. Experimental scheme of myeloid progenitor serial replating assay. *Hoxa9* was transduced in Figure 6B and *MLL-AF9* in Figure 6C and 6D. The time points at which colony forming units and *Hoxa9* expression were measured are shown. B. Clonogenic potentials of *Hoxa9*-transformed myeloid progenitors of wild type or *uc* homozygous mutant origin. CFUs per 10^4 plated cells were enumerated at third and fourth round. Error bars represent standard deviations of three independent samples. C. Clonogenic potentials of *MLL-AF9*-transformed myeloid progenitors of wild type or *uc* homozygous mutant origin. CFUs per 10^4 plated cells were enumerated at third and fourth round. Error bars represent standard deviations of three independent samples. D. *Hoxa9* expression in the first round colonies of *MLL-AF9*-transformed cells. Relative expression levels (normalized to *Gapdh*) and expressed relative to those of *MLL-AF9*-transformed wild type progenitors arbitrarily set as 100%. Error bars represent standard deviations of triplicate PCRs.
doi:10.1371/journal.pone.0073649.g006

the hematopoietic system, while a 10-fold lower cell number of the wild type/heterozygous control FL cells successfully reconstituted (Figure 2F). These results show that intra-molecular complex formation is essential for the functions of MLL to generate appropriate numbers of fetal HSCs and MPPs in vivo.

Proteolytic processing of MLL is not required for MLL-dependent gene activation

To investigate the in vivo roles of proteolytic processing of MLL, we generated a knock-in mouse line (designated *uc*) with targeted germline mutations of the MLL processing sites. ES cells were engineered to contain an alanine substitution mutation at the critical aspartic acid residue in both processing sites (the murine counterparts of human D2666 and D2718) [8], [10] thereby expressing an uncleavable mutant of MLL (MLL^{uc}) (Figure 3A). Genomic PCR followed by sequencing confirmed that recombined ES cells harbored the targeted allele (Figure 3B). Western blotting analysis confirmed expression of MLL^{uc} in *uc* mutant embryos (Figure 3C). *uc* homozygous mice were born at normal Mendelian ratios (Figure 3D) with no apparent anatomic/functional defects. *Hoxc8*, an MLL target gene [2], was properly expressed in *uc* homozygous embryos at E10.5, where *dC* homozygous embryos failed to maintain its expression [8] (Figure 3E). Thus, an inability to proteolytically process MLL does not compromise the developmental roles of MLL.

To further investigate the possible effect of MLL processing on MLL-dependent transcription, MEF cell lines of wild type, *uc* homozygous and *dC* homozygous genotypes were analyzed by RT-qPCR. In contrast to the comparable expression of *Mll* and *Hoxc4* mRNAs among all the cell lines, expression of MLL target genes including *Hoxc8*, *Hoxc9*, *Cdkn2c* and *Cdkn1b* [8], [22], [23] was substantially reduced in *dC* homozygous MEFs but unaffected in *uc* homozygous MEFs (Figure 3F). Although *Taspase I* knock-out MEFs, which exclusively express the unprocessed form of MLL, were reported to over-express *Cdkn2a*, *uc* homozygous MEFs expressed *Cdkn2a* at comparable levels to the wild type control, indicating that processing of MLL is not required for suppression of *Cdkn2a* expression. Furthermore, in contrast to a report by Takeda et al. [25], no severe growth retardation of *uc* homozygous MEFs was observed in proliferation assays and in 3T3 senescence assays, in the condition where *dC* homozygous MEFs displayed a premature senescence phenotype [8] (Figure 3G). Consistent with these results, *PAI-1* (also known as *Serpine-1*), a well-known senescence inducer [26], was highly expressed in *dC* homozygous MEFs, but expressed at normal levels in *uc* homozygous MEFs. Hence, processing of MLL is not required for MLL-dependent transcription in contrast to the severe compromise of MLL functions caused by the inability to self-associate.

Lack of MLL processing does not affect steady state hematopoiesis

To investigate the role of MLL processing in hematopoiesis, we analyzed the hematopoietic compartments of adult *uc* mutant mice by flow cytometry (Figure 4A, 4B). HSCs, MPPs, and lineage-restricted progenitors including common myeloid progenitors (CMPs), granulocyte/monocyte progenitors (GMPs) and mega-karyocyte/erythroid progenitors (MEPs) in bone marrow (BM) exhibited normal frequencies. Furthermore, T-cells in thymus, and B- cells in BM also exhibited normal compositions (data not

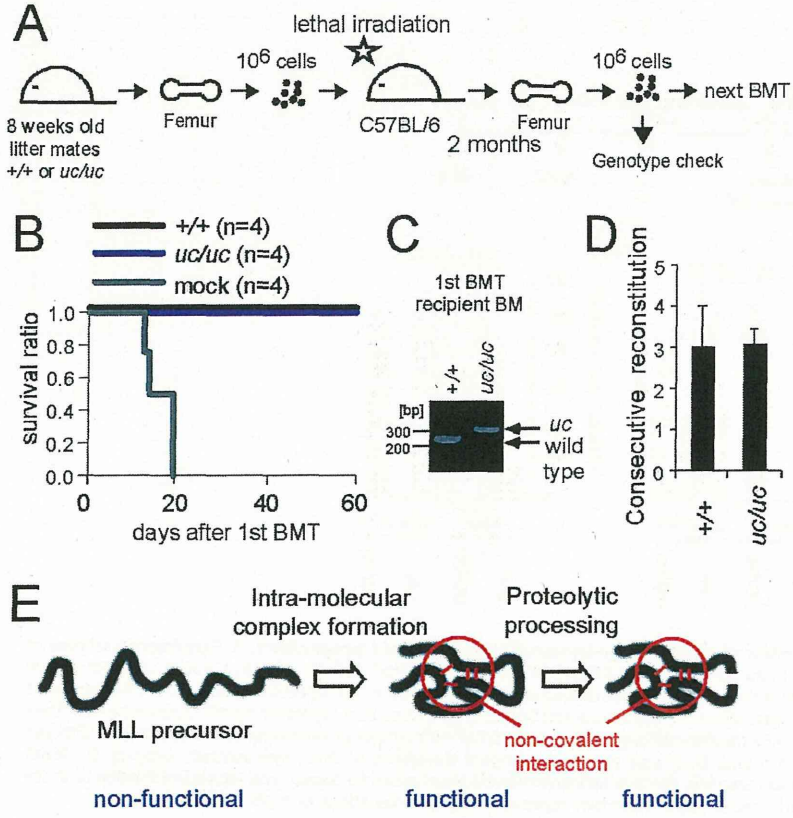

Figure 7. MLL processing is not required for self-renewal of hematopoietic stem cells. A. Experimental scheme of serial reconstitution assay. The time point at which the genotype of hematopoietic cells was examined is indicated. B. Survival of lethally irradiated mice transplanted with BM cells derived from adult *uc* homozygous mice and their littermate wild type control. Mock control mice die two to three weeks after irradiation. C. Genotype of reconstituted hematopoietic cells in the BM of recipient mice. The BM cells were prepared from femurs and subjected to genotyping PCRs. D. Reconstitution potentials of the donor cells before eventual exhaustion of HSCs. Recipient mice that survived for 60 days after transplantation were subjected to the next round of bone marrow transplantation (BMT). Average times of successful reconstitution were expressed with error bars that represent standard deviations of nine independent samples. E. Model of MLL protein maturation.
doi:10.1371/journal.pone.0073649.g007

shown). Thus, MLL processing is dispensable for steady-state hematopoiesis in adult mice.

The uncleavable mutant of MLL is not constitutively active

MLL maintains *HOX* gene expression to promote expansion of hematopoietic progenitors during myeloid differentiation [3], [4]. Because *Hox* gene expression progressively declines as cells differentiate [12], [27] (Figure 5A, upper panel), the transcriptional activity of MLL is presumed to decline in parallel. Transcripts for essential components of the MLL complex (MLL itself, menin and LEDGF) are also down-regulated as cells differentiate (Figure 5A, lower panel). However, their declining expression levels were not quantitatively in accord with those of *Hox* genes. Noticeably, their expression levels in differentiated cells ($ckit^{low}Mac1^{high}$) were similar to the levels present in *MLL-ENL*-transformed cells, whose growth is critically dependent on menin and LEDGF [28], [29], [30]. These data suggest that the decline of *Hox* gene expression during differentiation is not entirely due to the decrease of MLL complex components at the mRNA level; rather, a post-transcriptional regulatory mechanism might mediate down-regulation of MLL-dependent transcription. We hypothesized that dissociation of the MLL^C subunit may occur during differentiation to extinguish MLL function, whereas uncleavable MLL might function as the constitutively active form. In this scenario, myeloid progenitors derived from *uc* homozygous mice should exhibit enhanced clonogenicity in vitro similar to that induced by MLL-ENL, which behaves as the constitutively active form that aberrantly maintains *Hoxa9* expression and promotes proliferation (Figure 5B, 5C). However, *uc* homozygous myeloid progenitors did not display enhanced replating activity compared to the wild type control (Figure 5B, 5D). Thus, lack of processing does not render MLL constitutively active in hematopoietic progenitors.

MLL processing is not required for oncogene-dependent proliferation of myeloid progenitors

To examine whether MLL processing is required for the enhanced proliferation of hematopoietic progenitors induced by oncogenes, we transduced myeloid progenitors derived from *uc* homozygous mice with *Hoxa9* expression vector and analyzed their serial replating activity (Figure 6A). Despite the lack of processing, *Hoxa9*-transformed *uc* homozygous myeloid progenitors exhibited clonogenicity comparable to the wild type control (Figure 6B). These results demonstrate that MLL processing is not required for proliferation of oncogene-transformed myeloid progenitors.

It has been reported that the wild type MLL protein is required for leukemic transformation by the *MLL-AF9* oncogene [28]. This notion presumes that the function of MLL must be preserved for MLL-AF9 to activate *Hoxa9* expression and transform myeloid progenitors. MLL-AF9 successfully transformed *uc* homozygous myeloid progenitors (Figure 6C) and activated *Hoxa9* expression (Figure 6D) in a serial replating assay (Figure 6A). Hence, the uncleavable form of MLL is equivalently functional to the processed form of MLL in MLL-AF9-transformed myeloid progenitors.

MLL processing is not required for self-renewal of HSCs in vivo

Previous studies have shown that MLL serves an important role in self-renewal of HSCs and therefore is necessary to reconstitute the hematopoietic system in vivo [3], [7], [8] (Figure 2F). To examine the role of MLL processing in self-renewal, we performed serial in vivo reconstitution assays using wild type and *uc* homozygous donor cells derived from littermate mice (Figure 7A). *uc* homozygous BM cells successfully reconstituted the hematopoietic system as well as the wild type control (Figure 7B, 7C). Serial reconstitution assays showed that *uc* homozygous HSCs and the wild type control consecutively reconstituted three times on average before the eventual depletion of HSCs (Figure 7D), demonstrating that *uc* homozygous HSCs retain equivalent reconstituting potentials to the wild type control. These results indicate that MLL processing is not required for self-renewal of HSCs in vivo.

Discussion

In this study, we generated mouse mutant alleles that effectively inhibit intra-molecular complex formation and MLL processing, respectively, to address the in vivo roles of these two maturation steps. Loss of intra-molecular interaction had devastating effects and manifested a null phenotype, demonstrating that intra-molecular interaction of MLLN and MLLC is essential for MLL functions. These results indicate that loss of intra-molecular interaction exposes the FYRN domain, which triggers degradation and leads to loss-of-function of MLL as we previously reported [8]. On the other hand, in spite of the evolutionary conservation of the processing sites, loss of processing caused no measurable defects, indicating that processing is mostly dispensable for MLL-dependent functions. Furthermore, *uc* homozygous cells have normal proliferation capacity, demonstrated by proliferation assay of MEFs, serial replating assay of oncogene-transformed hematopoietic progenitors, and serial in vivo reconstitution assay. Therefore, our results do not support the previously suggested essential role of MLL processing in cell cycle progression. Taken together, MLL processing is not required for its function unlike many other bioactive peptides that become activated by proteolytic cleavage, whereas intra-molecular complex formation is an essential step in MLL maturation. Because cleavage occurs to the MLL mutant proteins that are incapable of intra-molecular interaction, the intra-molecular interaction itself is not a prerequisite for Taspase 1-dependent cleavage [8]. However, if cleavage occurs before the intra-molecular interaction, MLL fragments would dissociate from each other and be subjected to degradation. Hence, we propose a model in which intra-molecular interaction takes place first, followed by Taspase 1-dependent cleavage in the proper maturation process of MLL (Figure 7E).

Previous analysis of fetal and adult hematopoiesis showed that MLL is required for sufficient proliferative expansion of hematopoietic progenitors [3], [4], [7], [8]. During myeloid differentiation, MLL maintains expression of posterior *Hoxa* genes [3], [4], which are highly expressed in HSCs/MPPs and progressively down-regulated in more differentiated progenitors [12], [27] (Figure 4A). Posterior *Hoxa* genes are required to sufficiently promote proliferation of undifferentiated hematopoietic progenitors [5], [6], [12]. Hence, MLL-dependent *HOX* gene expression is necessary to maintain appropriate pool sizes of HSCs and immature progenitors. Our in vivo analyses of *uc* homozygous and *de* homozygous mutant mice show that intra-molecular complex formation but not MLL processing is required for proper expansion of hematopoietic progenitors. MLL fusion proteins generated by chromosomal translocations constitutively activate posterior *HOXA* genes to cause leukemia and therefore those mutations are defined as gain-of-function. Our analysis of *de* homozygous MEFs showed that loss of intra-molecular complex formation results in degradation of MLL proteins and impaired expression of MLL target genes. Thus, although deletion of exon 11 was originally found in ALL [21], this mutation is defined as loss-of-function, suggesting that this mutation likely contributes to leukemogenesis through different mechanisms from MLL fusion-dependent leukemogenesis.

MLL fragments generated by proteolytic processing associate with each other by non-covalent interaction, which potentially allows conditional dissociation of the MLL holocomplex. In accord with this hypothesis, genome wide ChIP analysis of Drosophila embryos showed that trithorax (TRX) protein fragments generated by processing differentially associate with the Drosophila genome [31]. Therefore, it was thought that MLL^C might dissociate from MLL^N in a context-dependent manner to become functionally inactive. In this scenario, the unprocessed mutant protein might function as the constitutively active form. However, unlike MLL fusion proteins, the uncleavable mutant did not enhance serial replating activity of hematopoietic progenitors (Figure 5D), indicating that conditional dissociation of MLL^C is not the major mechanism for extinguishing MLL activity during myeloid differentiation.

It has been proposed that MLL processing might be important for maintaining expression of the Antenapedia complex (ANT-C) genes. This concept was originated by the study of a Drosophila TRX mutant (trx^{E3}) that contains an internal deletion of amino acids encompassing the processing site and therefore exclusively expresses an uncleavable mutant protein [32], [33]. trx^{E3} exhibits mildly reduced ANT-C expression in late stages and normal bithorax complex (BX-C) expression, whereas the TRX null mutant (trx^{B11}) displays mildly decreased expression of ANT-C genes in late embryonic development and severely decreased expression of BX-C genes in early embryonic development. Thus, it was hypothesized that TRX processing might be required specifically for late ANT-C expression in fly embryonic development. However, our current results show that *uc* homozygous mice have no developmental defects. Furthermore, expression of *Hoxc4*, which is a member of the ANT-C genes, in *uc* homozygous MEFs was comparable to the wild type control (Figure 3F). Expression of *Hoxc8*, which is a member of the BX-C genes, was severely decreased in *dC* homozygous MEFs, but unaffected in *uc* homozygous MEFs. Thus, our results indicate that the role of MLL processing on *HOX* gene expression is minor, if any, in mammalian development.

Taspase 1 knock out mice demonstrate various defects including smaller body size, reduced MEF proliferation, and skeletal structural anomalies [25]. More specifically, Taspase 1 deficiency causes upregulation of CDK inhibitors such as p16 and ARF (the products of the *Cdkn2a* gene) to inhibit proliferation of MEFs. However, *uc* homozygous mice were born with normal body size,

and *uc* homozygous MEFs did not display severely altered expression of *Cdkn2a* (Figure 3F) nor manifested severe proliferation defects (Figure 3G) in contrast to a previous study that also analyzed mice engineered to express an uncleavable MLL protein [25]. The basis for these differences between the two independently generated mouse lines is unclear since detailed description of the mice generated by Takeda et al. was not reported [25], but may be due to differences in genetic backgrounds of the ES cells or the targeting vector. Nevertheless, our results indicate that MLL processing does not serve rate-limiting roles for proliferation and suggest that the growth defects caused by Taspase 1-deficiency may be attributed to other substrates such as MLL2 [25] or TFIIA [34].

Taken together, our results indicate that MLL processing has no biological roles in development, hematopoiesis and proliferation, whereas intra-molecular interaction of MLL is essential in all of those circumstances. However, evolutionary conservation of the processing sites suggests that MLL processing has some biological roles. It may be important under other circumstances not tested in this study such as stress conditions and immunity.

Conclusions

In the current study, we examined the in vivo roles of intra-molecular interaction and proteolytic processing of MLL in various assays. Loss of intra-molecular interaction caused loss-of-MLL function, whereas loss of processing caused no detectable functional alterations. These results unequivocally demonstrate that formation of an intra-molecular complex is, but the processing is not, required for MLL-dependent gene activation and cell proliferation.

Acknowledgments

We thank Drs. E. Allen and H. Zeng (Stanford Transgenic Research Facility) for technical support for the generation of knock-in mice, Drs. T. Yagi (Osaka University) and L. Selleri (Cornell University) for plasmids, and Dr. T. Kitamura (Tokyo University) for plat-E cells. We thank Drs. L. Selleri, T. Capellini (Cornell University) and J. Sage (Stanford University) for technical instruction and helpful discussion. We acknowledge C. Nicolas, M. Ambrus, B. T. Rouse, M. Shino and M. Kawaguchi for technical assistance.

Author Contributions

Conceived and designed the experiments: AY. Performed the experiments: AY FF MJM CM CH. Analyzed the data: AY FF MJM CM. Contributed reagents/materials/analysis tools: IK MLC. Wrote the paper: AY MLC.

References

1. Yu BD, Hanson RD, Hess JL, Horning SE, Korsmeyer SJ (1998) MLL, a mammalian trithorax-group gene, functions as a transcriptional maintenance factor in morphogenesis. Proc Natl Acad Sci U S A 95: 10632–10636.
2. Yu BD, Hess JL, Horning SE, Brown GA, Korsmeyer SJ (1995) Altered Hox expression and segmental identity in Mll-mutant mice. Nature 378: 505–508.
3. Jude CD, Climer L, Xu D, Artinger E, Fisher JK, et al. (2007) Unique and independent roles for MLL in adult hematopoietic stem cells and progenitors. Cell Stem Cell 1: 324–337.
4. Yagi H, Deguchi K, Aono A, Tani Y, Kishimoto T, et al. (1998) Growth disturbance in fetal liver hematopoiesis of Mll-mutant mice. Blood 92: 108–117.
5. Lawrence HJ, Christensen J, Fong S, Hu YL, Weissman I, et al. (2005) Loss of expression of the Hoxa-9 homeobox gene impairs the proliferation and repopulating ability of hematopoietic stem cells. Blood 106: 3988–3994.
6. Thorsteinsdottir U, Mamo A, Kroon E, Jerome L, Bijl J, et al. (2002) Overexpression of the myeloid leukemia-associated Hoxa9 gene in bone marrow cells induces stem cell expansion. Blood 99: 121–129.
7. McMahon KA, Hiew SY, Hadjur S, Veiga-Fernandes H, Menzel U, et al. (2007) Mll has a critical role in fetal and adult hematopoietic stem cell self-renewal. Cell Stem Cell 1: 338–345.
8. Yokoyama A, Ficara F, Murphy MJ, Meisel C, Naresh A, et al. (2011) Proteolytically cleaved MLL subunits are susceptible to distinct degradation pathways. J Cell Sci 124: 2208–2219.
9. Caslini C, Connelly JA, Serna A, Broccoli D, Hess JL (2009) MLL associates with telomeres and regulates telomeric repeat-containing RNA transcription. Mol Cell Biol 29: 4519–4526.
10. Smith LL, Yeung J, Zeisig BB, Popov N, Huijbers I, et al. (2011) Functional crosstalk between Bmi1 and MLL/Hoxa9 axis in establishment of normal hematopoietic and leukemic stem cells. Cell Stem Cell 8: 649–662.
11. Ayton PM, Cleary ML (2003) Transformation of myeloid progenitors by MLL oncoproteins is dependent on Hoxa7 and Hoxa9. Genes Dev 17: 2298–2307.
12. Krivtsov AV, Twomey D, Feng Z, Stubbs MC, Wang Y, et al. (2006) Transformation from committed progenitor to leukaemia stem cell initiated by MLL-AF9. Nature 442: 818–822.
13. Hsieh JJ, Cheng EH, Korsmeyer SJ (2003) Taspase1: a threonine aspartase required for cleavage of MLL and proper HOX gene expression. Cell 115: 293–303.
14. Hsieh JJ, Ernst P, Erdjument-Bromage H, Tempst P, Korsmeyer SJ (2003) Proteolytic cleavage of MLL generates a complex of N- and C-terminal fragments that confers protein stability and subnuclear localization. Mol Cell Biol 23: 186–194.
15. Yokoyama A, Kitabayashi I, Ayton PM, Cleary ML, Ohki M (2002) Leukemia proto-oncoprotein MLL is proteolytically processed into 2 fragments with opposite transcriptional properties. Blood 100: 3710–3718.
16. Ficara F, Murphy MJ, Lin M, Cleary ML (2008) Pbx1 regulates self-renewal of long-term hematopoietic stem cells by maintaining their quiescence. Cell Stem Cell 2: 484–496.
17. Capellini TD, Di Giacomo G, Salsi V, Brendolan A, Ferretti E, et al. (2006) Pbx1/Pbx2 requirement for distal limb patterning is mediated by the hierarchical control of Hox gene spatial distribution and Shh expression. Development 133: 2263–2273.
18. Sage J, Mulligan GJ, Attardi LD, Miller A, Chen S, et al. (2000) Targeted disruption of the three Rb-related genes leads to loss of G(1) control and immortalization. Genes Dev 14: 3037–3050.
19. Lavau C, Szilvassy SJ, Slany R, Cleary ML (1997) Immortalization and leukemic transformation of a myelomonocytic precursor by retrovirally transduced HRX-ENL. Embo J 16: 4226–4237.
20. Yokoyama A, Lin M, Naresh A, Kitabayashi I, Cleary ML (2010) A higher-order complex containing AF4 and ENL family proteins with P-TEFb facilitates oncogenic and physiologic MLL-dependent transcription. Cancer Cell 17: 198–212.
21. Lochner K, Siegler G, Fuhrer M, Greil J, Beck JD, et al. (1996) A specific deletion in the breakpoint cluster region of the ALL-1 gene is associated with acute lymphoblastic T-cell leukemias. Cancer Res 56: 2171–2177.
22. Milne TA, Briggs SD, Brock HW, Martin ME, Gibbs D, et al. (2002) MLL targets SET domain methyltransferase activity to Hox gene promoters. Mol Cell 10: 1107–1117.
23. Milne TA, Hughes CM, Lloyd R, Yang Z, Rozenblatt-Rosen O, et al. (2005) Menin and MLL cooperatively regulate expression of cyclin-dependent kinase inhibitors. Proc Natl Acad Sci U S A 102: 749–754.
24. Kim I, He S, Yilmaz OH, Kiel MJ, Morrison SJ (2006) Enhanced purification of fetal liver hematopoietic stem cells using SLAM family receptors. Blood 108: 737–744.
25. Takeda S, Chen DY, Westergard TD, Fisher JK, Rubens JA, et al. (2006) Proteolysis of MLL family proteins is essential for taspase1-orchestrated cell cycle progression. Genes Dev 20: 2397–2409.
26. Kortlever RM, Higgins PJ, Bernards R (2006) Plasminogen activator inhibitor-1 is a critical downstream target of p53 in the induction of replicative senescence. Nat Cell Biol 8: 877–884.
27. Somervaille TC, Cleary ML (2006) Identification and characterization of leukemia stem cells in murine MLL-AF9 acute myeloid leukemia. Cancer Cell 10: 257–268.
28. Thiel AT, Blessington P, Zou T, Feather D, Wu X, et al. (2010) MLL-AF9-induced leukemogenesis requires coexpression of the wild-type Mll allele. Cancer Cell 17: 148–159.
29. Yokoyama A, Cleary ML (2008) Menin critically links MLL proteins with LEDGF on cancer-associated target genes. Cancer Cell 14: 36–46.
30. Yokoyama A, Somervaille TC, Smith KS, Rozenblatt-Rosen O, Meyerson M, et al. (2005) The menin tumor suppressor protein is an essential oncogenic cofactor for MLL-associated leukemogenesis. Cell 123: 207–218.
31. Schuettengruber B, Ganapathi M, Leblanc B, Portoso M, Jaschek R, et al. (2009) Functional anatomy of polycomb and trithorax chromatin landscapes in Drosophila embryos. PLoS Biol 7: e13.
32. Mazo AM, Huang DH, Mozer BA, Dawid IB (1990) The trithorax gene, a trans-acting regulator of the bithorax complex in Drosophila, encodes a protein with zinc-binding domains. Proc Natl Acad Sci U S A 87: 2112–2116.

33. Sedkov Y, Tillib S, Mizrokhi L, Mazo A (1994) The bithorax complex is regulated by trithorax earlier during Drosophila embryogenesis than is the Antennapedia complex, correlating with a bithorax-like expression pattern of distinct early trithorax transcripts. Development 120: 1907–1917.

34. Zhou H, Spicuglia S, Hsieh JJ, Mitsiou DJ, Hoiby T, et al. (2006) Uncleaved TFIIA is a substrate for taspase 1 and active in transcription. Mol Cell Biol 26: 2728–2735.

Regular Article

TRANSPLANTATION

Quantitation of hematogones at the time of engraftment is a useful prognostic indicator in allogeneic hematopoietic stem cell transplantation

Takahiro Shima,[1,2] Toshihiro Miyamoto,[1] Yoshikane Kikushige,[1,2] Yasuo Mori,[1,2] Kenjiro Kamezaki,[1] Ken Takase,[3] Hideho Henzan,[3] Akihiko Numata,[3] Yoshikiyo Ito,[4] Katsuto Takenaka,[1] Hiromi Iwasaki,[2] Tomohiko Kamimura,[4] Tetsuya Eto,[3] Koji Nagafuji,[1] Takanori Teshima,[2] Koji Kato,[1] and Koichi Akashi[1,2]

[1]Department of Medicine and Biosystemic Science and [2]Center for Cellular and Molecular Medicine, Graduate School of Medical Sciences, Kyushu University Graduate School of Medicine, Fukuoka, Japan; [3]Department of Hematology, Harasanshin Hospital, Fukuoka, Japan; and [4]Department of Hematology, Hamanomachi General Hospital, Fukuoka, Japan

Key Points

- Quantitation of hematogones at engraftment is useful to predict prognosis of patients treated with allogeneic stem cell transplantation.

Transient marrow expansion of normal B-cell precursors, termed hematogones, is occasionally observed after hematopoietic stem cell transplantation (HSCT). To understand the clinical significance of this phenomenon, we enumerated hematogones in 108 consecutive patients who received allogeneic HSCT for the treatment of hematologic malignancies, including acute myelogenous leukemia, advanced myelodysplastic syndromes, acute lymphoblastic leukemia, and non-Hodgkin lymphoma. Hematogone quantitation was performed at the time of complete donor engraftment (median day 25 and 32 in patients who received bone marrow and cord blood cell transplants, respectively). Hematogones were polyclonal B cells, and their frequencies correlated positively with blood B-cell numbers, and inversely with donors' but not recipients' age, suggesting that hematogones reflect cell-intrinsic B-cell potential of donor cells. Interestingly, patients developing hematogones that comprised > 5% of bone marrow mononuclear cells constituted a group with significantly prolonged overall survival and relapse-free survival, irrespective of their primary disease or donor cell source. In addition, patients with > 5% hematogones developed severe acute graft-versus-host diseases less frequently, which may contribute toward their improved survival. We therefore conclude that the amount of hematogones at the time of engraftment may be a useful tool in predicting the prognosis of patients treated with allogeneic HSCT. (*Blood.* 2013;121(5):840-848)

Introduction

Hematogones are transient increases in lymphoblast-looking cells in the bone marrow.[1,2] Because of the morphologic resemblance between residual leukemic clones and hematogones, expansion of hematogones during the recovery phase from chemotherapy and bone marrow transplantation occasionally causes diagnostic confusion.[1-3] Phenotypic analyses have demonstrated that hematogones are normal B-cell precursors, including pro-B, pre-B, and immature B cells coexpressing CD10 and CD19.[1,2] The fact that hematogones become prominent in the recovery phase after chemotherapy or hematopoietic stem cell transplantation (HSCT)[1-6] suggests that they could reflect active B-cell reconstitution. They are also sometimes seen in steady-state hematopoiesis, especially in healthy infants and young people.[2,4,7,8] Previous work demonstrated that in the recovery phase after chemotherapy, the percentage of hematogones in the bone marrow was inversely correlated with patients' age.[1] However, it is unclear whether the age-associated decline in hematogones frequency reflects cell-intrinsic defects of hematopoietic stem cell activity or cell-extrinsic defects such as aging of the bone marrow microenvironment.

Recent reports have shown that hematogone expansion correlates with favorable outcomes in acute myelogenous leukemia (AML) patients treated with chemotherapy[5] or cord blood transplantation (CBT).[6] However, the precise number or frequency above which hematogones correlate with clinical significance has not been clarified. Previous reports[1,5,6] have reported hematogone frequency relative to bone marrow mononuclear cells (MNCs), total nuclear cells (TNCs), and frequencies of B-cell precursors, and as a result, hematogone expansion has been described with frequencies ranging from > 0% to 0.9%.[1,5,6]

To better understand the etiology and clinical significance of hematogones, we measured percentages of B-cell precursors in the bone marrow via flow cytometry in 108 consecutive patients with hematologic malignancies, including AML, advanced myelodysplastic syndromes (MDS), acute lymphoblastic leukemia (ALL), and lymphoma, who achieved successful engraftment after allogeneic HSCT at our institution. The analysis of hematogones was performed on the day of engraftment, defined as the day when circulating granulocytes reached > 0.5×10^9/L for 3 consecutive days,[9-12] and the bone marrow showed complete donor-type chimerism via polymerase chain reaction (PCR) analysis. To minimize the effect of expanding granulocytes on hematogone frequencies, bone marrow MNCs were used for flow cytometric

Submitted February 7, 2012; accepted November 19, 2012. Prepublished online as *Blood* First Edition paper, December 11, 2012; DOI 10.1182/blood-2012-02-409607.

The online version of this article contains a data supplement.

The publication costs of this article were defrayed in part by page charge payment. Therefore, and solely to indicate this fact, this article is hereby marked "advertisement" in accordance with 18 USC section 1734.

Table 1. Patients' characteristics

	BMT: no. (%), [range]	CBT: no. (%), [range]	Total (%)	*P*
Recipient sex, male/female	35 (32)/24 (22)	26 (24)/23 (21)		NS
Recipient age, y	49.2 (mean) [20-66]	47.3 (mean) [19-67]		NS
Donor sex, male/female	37 (34)/22 (20)	24 (22)/25 (23)		NS
Donor age, y	36.7 (mean) [17-66]	0		< .001
No. of infused cell, /kg	2.80×10^8 (mean) [0.92-4.02]	0.28×10^8 (mean) [0.18-0.50]		< .001
Primary disease				NS
AML/advanced MDS				
CR	14 (13)	11 (10)	25 (23)	
non-CR	21 (19)	14 (13)	35 (32)	NS
Total	35 (32)	25 (23)	60 (56)	
ALL				
CR	3 (3)	3 (3)	6 (6)	
non-CR	2 (2)	10 (9)	12 (11)	NS
Total	5 (5)	13 (12)	18 (17)	
Lymphoma				
CR	7 (6)	3 (3)	10 (9)	
non-CR	12 (11)	8 (7)	20 (19)	NS
Total	19 (18)	11 (10)	30 (28)	
Conditioning regimen				< .01
TBI/CY	28 (26)	24 (22)		
BU/CY	14 (13)	0 (0)		
RIC	17 (16)	25 (23)		
GVHD prophylaxis				< .001
TAC + sMTX	51 (47)	6 (6)		
CSP + sMTX	8 (7)	28 (26)		
CSP + MMF	0 (0)	15 (14)		
HLA disparity				< .001
6/6	39 (36)	1 (1)		
5/6	20 (19)	7 (6)		
4/6	0 (0)	22 (20)		
3/6	0 (0)	19 (18)		
Days required for engraftment	25 (median) [15-32]	32 (median) [14-39]		< .01

ALL indicates acute lymphoblastic leukemia; AML, acute myelogenous leukemia; BMT, bone marrow transplantation; BU, busulfan; CBT, cord blood transplantation; CR, complete remission; CSP, cyclosporine; CY, cyclophosphamide; GVHD, graft- versus-host disease; MDS, myelodysplastic syndrome; MMF, mycophenolate mofetil; NS, not significant; RIC, reduced-intensity conditioning; sMTX, short-term methotrexate; TAC, tacrolimus; and TBI, total body irradiation.

analyses in all cases. Our data suggest that the number of hematogones generally reflects cell-intrinsic B-cell potential of donor hematopoietic stem cells (HSCs) and that this declines with aging. We also found that hematogone frequencies of > 5% of total MNCs is a useful cutoff line to distinguish patient groups with significantly better overall survival (OS) or with relapse-free survival (RFS), irrespective of their primary diseases or donor cell sources. We propose that the quantitation of hematogones at engraftment may be useful to predict the prognosis of patients treated with allogeneic HSCT.

Methods

Patients

From 2005 to 2010, 134 patients with high-grade hematologic malignancies were treated with allogeneic HSCT in Kyushu University Hospital. These patients included AML cases with high risk,[13] relapsed or refractory status, advanced MDS cases with intermediate-II or high risk on International Prognostic Scoring System classification,[14,15] ALL cases with high risk,[16] relapsed or refractory status, and relapsed non-Hodgkin lymphoma cases. Within these 134 patients, grafts were rejected in 5 cases and residual malignant cells proliferated soon after HSCT in 21 cases, without achieving successful engraftment. The remaining consecutive 108 cases, in which allogeneic HSCT was successful and complete donor-type chimerism was documented, were enrolled in this study. Fifty-nine and 49 patients received bone marrow transplantation (BMT) and CBT, respectively. Patients' characteristics are summarized in Table 1. This study was approved by the institutional review board of Kyushu University Hospital and conducted in accordance with the Declaration of Helsinki.

Evaluation of remission status before HSCT

Before HSCT, patients were intensively searched for residual malignant cells to define their pretransplantation remission status. In acute leukemia or advanced MDS cases, bone marrow samples were checked first by microscopic analysis, and were subjected to multicolor flow cytometric analysis.[13,17] Complete remission (CR) was diagnosed when percentages of cells of leukemia phenotype were < 0.5% in the bone marrow. Furthermore, 21 patients with acute leukemia or MDS had leukemia-specific genes such as BCR-ABL, FLT3-ITD, AML1-ETO, and MLL fusions, and PCR amplification of these genes were used to detect minimal residual disease (MRD).[13] Within these 21 patients, 17 patients were diagnosed as CR based on flow cytometric analyses. CR results for these 17 patients were also confirmed by PCR. In lymphoma patients, remission status was defined by evaluating the involvement of lymphoid organs using FDG-PET CT scan and/or MRI methods, and was also defined by evaluating the involvement of bone marrow by flow cytometry, as previously described.[18]

Transplantation procedures

Patients' characteristics were not statistically different between BMT and CBT recipient groups in terms of sex, age, and primary disease (Table 1). Conditioning regimen consisted of total body irradiation/cyclophosphamide (CY) for 28 BMT and 24 CBT recipients, busulfan (BU)/CY for 14 BMT recipients, and fludarabine-based reduced-intensity conditioning[19,20] for 17 BMT and 25 CBT recipients, respectively (Table 1).

Prophylaxis for graft-versus-host disease (GVHD) was tacrolimus/short-term methotrexate (sMTX) for 51 BMT and 6 CBT recipients, cyclosporine (CSP)/sMTX for 8 BMT and 28 CBT recipients, and CSP/mycophenolate mofetil for 15 CBT recipients (Table 1). The mean number of donor cells transplanted was 2.8×10^8/kg in BMT recipients and 0.28×10^8/kg in CBT recipients. Bone marrow units were obtained from the Japan Marrow Donor Program or related donors, and cord blood units were obtained from the Japanese Cord Blood Bank Network.

Evaluation for engraftment

The bone marrow sampling for the analysis of hematogones was performed when patients achieved successful engraftment. The standard criterion for engraftment was used according to previous studies.[9-12] Blood neutrophil numbers were checked daily after transplantation, and the successful engraftment was defined when neutrophils exceeded 0.5×10^9/L for 3 consecutive days. When patients met the criteria for engraftment, host/donor microchimerism analysis was performed (see the next section). If the analysis showed complete donor type chimerism, hematogones in the bone marrow were counted by multicolor flow cytometric analysis.

Chimerism analysis

To analyze donor/recipient cell chimerism, PCR amplification of polymorphic short tandem repeats (STR) was performed to confirm engraftment of donor cells. PCR using synthesized oligonucleotide templates were performed using TAKARA *Taq* Reagent Kits and run in the Perkin Elmer GeneAmp PCR system 9600 or 2400. The donor-cell origin and recipient-cell origin PCR product mixture was loaded onto the 373A sequencer (Applied Biosystems) with a size marker, and the data were processed using the GeneScan software (Applied Biosystems) as described previously.[21]

Flow cytometry analysis and cell sorting

The bone marrow mononuclear cells were prepared by the gradient centrifugation method as previously described.[22,23] Cells were stained with allophycocyanin-conjugated anti-CD34 (BD Pharmingen), biotin-conjugated anti-CD38 (Caltag Laboratories), FITC-conjugated anti-CD10 (DAKO), PE-conjugated anti-CD20 (BD Biosciences), PE-Cy7–conjugated anti-CD19 (BioLegend), and Cy5-PE–conjugated lineage (Lin) mixture (anti-CD3, -CD4, -CD8 (BD Pharmingen) -CD11b (Caltag Laboratories), -CD14, and -CD56 (Beckman Coulter).[22-25] Streptavidin-conjugated Cy7-allophycocyanin (BD Pharmingen) was used for visualization of biotinylated antibodies. For analysis of mature B cells, peripheral blood (PB) cells were stained with FITC-conjugated anti-CD10 (DAKO), PE-conjugated anti-CD20 (BD Biosciences), PE-Cy7–conjugated anti-CD19 (BioLegend), and Cy5-PE–conjugated Lin mixture. Available PB cells at day 90 after HSCT could be obtained from 64 patients and evaluated. Cells were analyzed by using a FACSAria (BD Biosciences) or FACSCanto (BD Biosciences). Cell sorting was performed on a 5-color FACSAria (BD Biosciences). To minimize contamination, cells were collected after the second round of sorting using sorting gates identical to those used in the first-round sorting. Definition of hematogones is a series of normal B-lymphoid precursors, including $CD34^+CD38^+CD10^+CD19^+Lin^-$ pro-B cells, $CD34^{-/lo}CD38^+CD10^+CD19^+$ pre-B cells, and $CD34^-CD38^+CD10^+CD19^+$ $CD20^+$ immature B cells[26-28] in bone marrow MNCs. Isotype controls were used to define the cutoff of positivity of each antigen on a FACS.

PCR analysis of *IGH* gene rearrangement

To analyze clonality of *IGH* gene rearrangements status of hematogones, DNA was obtained from 10 000 double-sorted cells[22,23,29] from all recipients presenting > 0.1% MNCs of hematogones on FACS. Then PCR amplification of DJ_H and VDJ_H gene rearrangement was performed as described previously.[24,30]

Statistical analysis

Relationships of percentages of hematogones with age, the day of engraftment, and numbers of circulating B lymphocytes were analyzed with the Spearman rank correlation analysis. Comparison between 2 groups or condition was tested with the Mann-Whitney U test. The categorical variables were analyzed with the 2-tailed χ^2 test. Survival was plotted with Kaplan-Meier curves, taking the interval from date of HSCT to death/relapse or last contact. Comparisons between each group were performed with the log-rank test and the Cox proportional hazards model. Univariate analysis was performed with logistic or exact logistic regression, and the parameters that present $P < .20$ were reevaluated by multivariate analysis.[31] Multivariate analysis was performed with logistic regression applying Firth's bias reduction. A P value $< .05$ was considered to be statistically significant.

Results

Hematogones that appeared at the time of engraftment are polyclonal B-cell precursors

One hundred eight consecutive cases treated with successful allogeneic BMT or CBT were enrolled in this study. Hematogones in the bone marrow were counted on the day of engraftment by multicolor flow cytometric analysis. The successful engraftment was judged when neutrophils exceeded $> 0.5 \times 10^9$/L for 3 consecutive days.[9-12] At this phase, it is critical to exclude residual leukemic cells or host-derived B-cell precursors from a cell fraction of hematogones. To this end, polymorphic STR was amplified to test the host/donor microchimerism, and only when patients' bone marrow consisted of 100% donor-derived cells, the analysis of hematogones was performed. The complete donor-type chimerism verifies that host-derived normal hematopoietic cells and malignant leukemic cells have been eliminated below the sensitivity of FACS,[32-34] and therefore that phenotypically defined hematogones in these patients on FACS were donor-derived normal cells.

Hematogones were morphologically blastic cells (Figure 1A), and were identified by surface phenotype, according to the definition of pro-B, pre-B, and/or immature B cells that coexpress CD10 and CD19 on their cell surface[1,26-28] (Figure 1B). To minimize the effect of granulocytes on hematogone frequencies, we used MNCs instead of TNCs in our analysis. The frequencies of hematogones in MNCs are usually higher than those in TNCs (not shown), as reported previously.[1]

The time median to engraftment was 25 and 32 days in patients treated with BMT and CBT, respectively (Table 1). The time required for engraftment appears to be consistent with previous reports.[34-39] Percentages of B-cell precursors within the bone marrow MNCs at the time of complete donor-type engraftment were significantly higher in CBT recipients than in BMT recipients (6.37% vs 1.75%; $P < .001$; Figure 1C). There was no significant relationship between the day of engraftment (the day of sampling) and the frequency of hematogones (Figure 1D).

In 106 of 108 patients who had > 0.1% of B-cell precursors in the bone marrow MNCs, B-cell precursors were purified by a multicolor FACS and were subjected to *IGH* rearrangement analysis. In all of these patients, B-cell precursors were polyclonal based on the rearrangement analysis of the *IGH* genes (Figure 1E).

Hematogones generally represent B-cell recovery potential of the graft and their emergence is related to age of donors but not recipients

Because hematogones are normal B-cell precursors, we tested whether the presence of a high number of them could reflect the active B-cell recovery after HSCT. FACS analysis of circulating blood cells revealed that the frequency of bone marrow B-cell precursors was significantly correlated with the number of blood

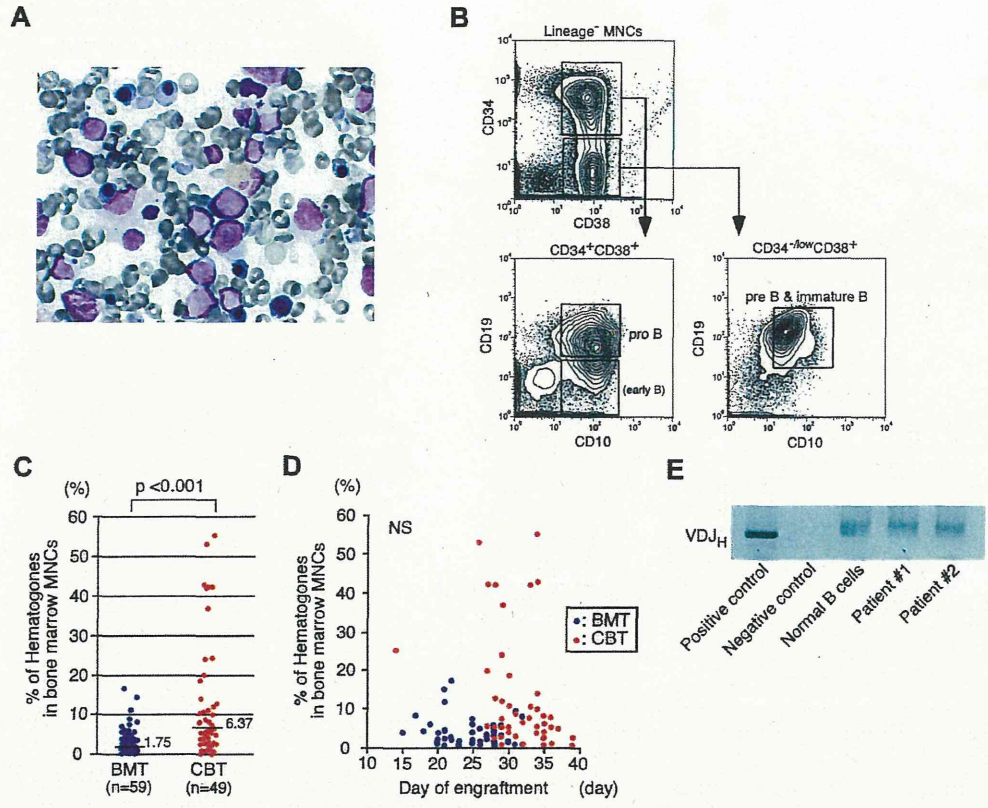

Figure 1. Detection of hematogones after allogeneic HSCT. (A) Typical appearance of hematogones in the bone marrow after HSCT (Giemsa staining ×1000; OLYMPUS BH-2 microscope [Olympus]; ACT-2U imaging software [Nikon]; 27°C). (B) Evaluation of hematogones on a 5-color FACS. Hematogones are defined as MNCs coexpressing CD10 and CD19 in the bone marrow at engraftment. They include $CD34^+CD38^+CD10^+CD19^+Lin^-$ pro-B cells, $CD34^{-/lo}CD38^+CD10^+CD19^+$ pre-B cells, and $CD34^-CD38^+CD10^+CD19^+CD20^+$ immature B cells. (C) Percentage of hematogones in the bone marrow MNCs in patients who received BMT and CBT. CBT recipients presented much higher frequency of hematogones compared with BMT recipients ($P < .001$). Solid bars indicate the median percentage of hematogones for each recipient; MNC, mononuclear cells; BMT, bone marrow transplantation; and CBT, cord blood transplantation. (D) The relationship between the day of engraftment and percentages of hematogones. There was no relationship between these parameters. (E) *IGH* rearrangement analysis of purified hematogones. B-cell precursors were polyclonal in all 106 recipients analyzed.

B cells at the time of engraftment ($R = 0.47$, $P < .001$; Figure 2A), and with those even on day 90 after HSCT ($R = 0.22$, $P < .01$; Figure 2B). These results suggest that expansion of hematogones reflects not only enhanced B-cell reconstitution potential of the graft, but also prolonged B cell–producing capability of donor HSCs.

The age of BMT donors ranged from 17 to 66 years old (median, 37 years; Table 1). Interestingly, there was a significant inversed correlation between donor age and percentage of bone marrow hematogones in patients treated with BMT ($R = 0.32$, $P = .02$; Figure 2C blue line). When the age of CBT donors were defined as 0-year old, the significant inversed correlation between age and hematogone numbers was also found in all patients entered in this study ($R = 0.42$, $P < .001$; Figure 2C black line). In contrast, recipients' age and hematogone numbers did not show any relationship (Figure 2D). Furthermore, as shown in Table 2, the time of engraftment was not affected by primary diseases of patients, or by their remission status at the time of HSCT. Thus, although the patients who fail to achieve CR are usually treated with higher total doses of chemotherapeutic drugs because of their refractory disorders, it did not affect the day of engraftment or the day of hematogone analysis for this study. These data strongly suggest that the number of hematogones after HSCT generally reflects the cell-intrinsic B-cell recovery potential of donor HSCs, which may decline by aging.

The emergence of hematogones up to > 5% of MNCs in the bone marrow represents a good prognosis for patients treated with allogeneic HSCT

It should be critical to draw a line of hematogone numbers to distinguish a group of patients with clinical significance. Therefore, we first compared the OS and RFS among patient subgroups with ≤ 1%, 1%-2%, 2%-3%, 3%-4%, 4%-5%, or > 5% of hematogones in our study (Figure 3A-B). Strikingly, patients who developed hematogones up to > 5% of MNCs showed significantly better 3-year OS (100%) and RFS (93.3%), compared with any other group. Patient groups with ≤ 1%, 1%-2%, 2%-3%, and 3%-4% of hematogones showed similar 3-year OS and RFS that were 37%-53% and 22%-51%, respectively. Interestingly, patients with 4%-5% hematogones appeared to show intermediate levels of OS (86%) and RFS (64%), although this is not statistically better than those in patients with ≤ 1% hematogones (Figure 3A-B). Based on these results, we hypothesized that the development of > 5% of hematogones might be critical to distinguish a patient group with favorable prognosis.

According to this criteria, 43 patients developed > 5% MNCs of hematogones (HG^+) and the remaining 65 patients had ≤ 5% MNCs of hematogones (HG^-). As shown in Figure 3A, in HG^+ patients, 3-year OS was 100%, whereas in HG^- patients, it was 45% ($P < .001$). The favorable OS in HG^+ groups is at least

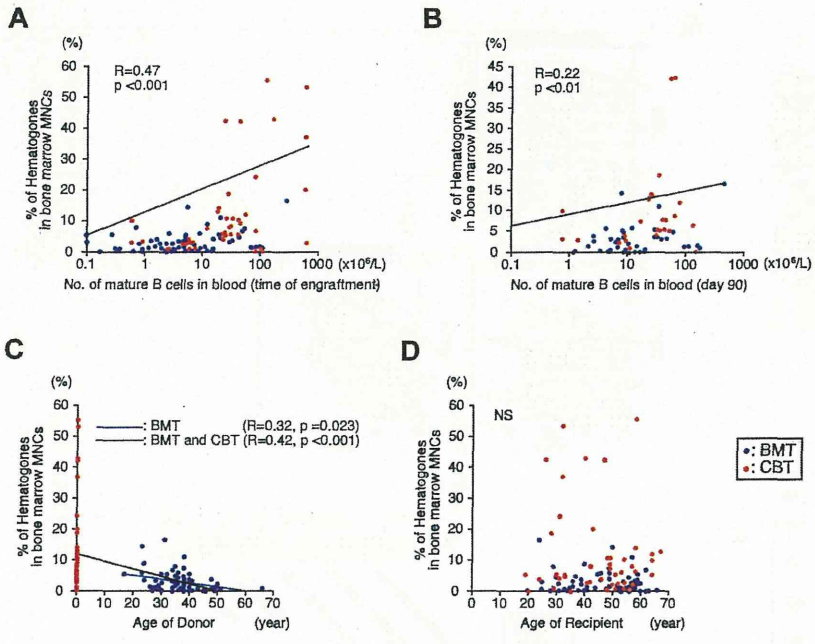

Figure 2. Analysis of hematogones, and the correlation of their frequency compared with blood B-cell numbers and age of donors. (A) A relationship between frequencies of hematogones and blood B cells at engraftment ($P < .001$). (B) A relationship between frequencies of hematogones at engraftment and blood B cells on day 90 ($P < .01$). (C) A relationship between frequency of hematogones and donor's age in patients who received BMT (blue line, $P = .023$), and in all recipients treated with either BMT or CBT (black line, $P < .001$). (D) No significant relationship was observed between frequency of hematogones and recipient age. NS indicates not significant.

because of the less frequent disease relapse. As shown in Figure 3B, significant association was observed between the presence of hematogones and 3-year RFS after HSCT: 3-year RFS was 93% and 37% in HG^+ and HG^- patients, respectively ($P < .001$). The association between the presence of > 5% hematogones and favorable OS and RFS was also seen when the analysis was performed in patient subgroups that received either BMT or CBT (Figure 3C-D). These data strongly suggest that the emergence of hematogones is a useful predictor of favorable outcomes at least in terms of OS and RFS, irrespective of donor cell source.

The emergence of hematogones (> 5% of MNCs) marks favorable outcomes for allogeneic HSCT especially in patients who failed to achieve complete remission, irrespective of primary malignant disease

We then analyzed whether the good prognosis designated by the emergence of hematogones is dependent on the primary malignant disorder. The OS and RFS were analyzed in each patient group with AML/advanced MDS, ALL, or non-Hodgkin lymphoma. As shown in Figure 4, HG^+ patients always showed significantly better OS and RFS compared with HG^- patients, in any of these patients groups suffering from different primary diseases.

It is well known that the achievement of CR at the time of transplantation favorably affects the prognosis after allogeneic HSCT.[13] Interestingly, in AML/advanced MDS patients, the HG^+ group showed significantly prolonged OS and RFS compared with the HG^- group, irrespective of their remission status at HSCT (Figure 5). The similar analysis was performed in ALL and lymphoma patient groups (supplemental Figure 1, available on the *Blood* Web site; see the Supplemental Materials link at the top of the online article). Although each group contained only a limited number of patients, statistically significant prolonged OS and RFS were also seen in patients who did not achieve CR at HSCT in both the ALL and the lymphoma patient groups.

Thus, the appearance of hematogones might mark favorable OS and RFS regardless of their primary malignancy.

Expansion of hematogones is frequently observed in patients who did not develop infection or severe acute GVHD

In this study, all 43 HG^+ patients are currently alive, although primary diseases have relapsed in 3 patients. In contrast, 32 of 65 HG^- patients have died. The causes of death in these 32 HG^- patients are shown in Table 3. Twenty-six patients died of their refractory primary disease, and 6 patients died of TRM, including

Table 2. Time required for engraftment in patients grouped by their primary disease or complication of infection or acute GVHD

		Time required for engraftment, d					
		BMT			CBT		
Disease	Remission status	No.	Mean, d	*P*	No.	Mean, d	*P*
AML and advanced MDS	CR/non-CR	14/21	27.0/24.4	.11	11/14	31.5/31.8	.37
ALL	CR/non-CR	3/2	23.7/29.5	.35	3/10	34.3/32.1	.45
Lymphoma	CR/non-CR	7/12	26.1/22.8	.10	3/8	33.0/29.3	.44
			Overall	.10		Overall	.53
After HSCT							
Infections	Yes/No	38/21	25.3/24.8	.66	22/27	30.8/32.2	.61
Acute GVHD	Grade II-IV/Grade 0-I	26/33	24.7/25.3	.25	14/35	32.3/31.3	.47

ALL indicates acute lymphoblastic leukemia; AML, acute myelogenous leukemia; BMT, bone marrow transplantation; CBT, cord blood transplantation; CR, complete remission; GVHD, graft-versus-host disease; HSCT, hematopoietic stem cell transplantation; and MDS, myelodysplastic syndrome.